

CLEARED  
FOR PUBLIC RELEASE

PL/PH 16 DEC 96

Sensor and Simulation Notes

Note 140

October 1971

Electromagnetic Interaction Between a Perfectly Conducting Sphere  
and a Two-Parallel-Plate Simulator, I (Top Plate Removed)

by

A. D. Varvatsis and M. I. Sancer  
Northrop Corporate Laboratories  
Pasadena, California

Abstract

The proximity effect is studied of a perfectly conducting plate on the response of a perfectly conducting sphere illuminated by a monochromatic plane wave or a step-function pulse. Numerical results are obtained for the frequency and time response of the charge densities on the poles of the sphere and of the total current crossing the equator.

DL-96-1955

### Acknowledgment

We thank Mr. R. W. Sassman for his invaluable assistance in numerical computation, Dr. Carl Baum for his helpful comments and Mrs. Georgene Peralta for her skillful and efficient typing.

## I. Introduction

In this note we examine the interaction of a plane electromagnetic wave or a step-function pulse with a perfectly conducting sphere within a two-parallel-plate simulator. In particular we focus our attention on the special case where the sphere has a diameter much smaller than the plate separation and is situated close to the bottom plate. We idealize this problem by completely removing the top plate. In a future note we will consider the two-plate interaction problem. The interaction of a test object within a two-parallel-plate simulator with an incident wave has been studied before in both the static and dynamic regimes. The test object has been taken to be a cylinder of finite length (Ref. 1, 2, 3, 4, 5, 6) or infinite length (Ref. 7). Returning to the special problem where the sphere is situated above a perfectly conducting plate and is illuminated by an incident wave, we can use the method of images to arrive at the interaction problem involving two perfectly conducting spheres of equal radius. Studies of the multiple scattering of an incident wave by two spheres exist in the literature (see for example Ref. 8, 9, 10, 11). The quantities of interest in these studies are the scattered field and the back-scattering cross section. In this note we are primarily interested in the proximity effect of the plate on the sphere. Thus, in studying this effect we can select some specific quantities the knowledge of which requires a relatively simple formulation. These quantities are the charge densities on the north and south poles and the total current crossing the equator. The knowledge of the charge densities at these points furnishes information about the local interaction in the immediate vicinity of the plates, whereas the knowledge of the current provides an overall picture of the effect of the plates on the interaction problem. Our formulation consists of deriving an integral equation for the  $\phi$  independent component of the current density. The angle  $\phi$  is the azimuthal angle in a spherical coordinate system with the  $z$  axis piercing through the south and north poles. The quantities of interest previously mentioned, that is, the charge densities on the north and south poles and the total current can be derived from a knowledge of the  $\phi$  independent current density.

In section II we give a formulation for the general interaction problem involving a perfectly conducting body within a two-parallel-plate simulator.

This is done by deriving an integral equation for the current density on the conducting body. Next we specialize to the sphere case and we present an integral equation for the  $\phi$  independent current density. Finally, we remove the top plate and focus our attention on the one-plate problem. We solve the integral equation in the frequency domain numerically on a computer, and we obtain the time response to an incident step-function pulse by numerical Fourier inversion. In section III, we discuss the interrelationship between high and low-frequency behavior to early and late-time behavior. In section IV we discuss the plots of the quantities of interest in the frequency and time domain and ascertain the importance of the proximity effect of the plate.

## II. Formulation of the Problem

In general one has to solve the problem of the scattering of a plane monochromatic wave by a conducting body positioned between two parallel conducting plates of infinite extent (Fig. 1). An integral equation approach for the current induced on the conducting body is feasible through the use of a dyadic Green's function satisfying appropriate boundary conditions on the plates. We start from the pair of equations

$$\nabla \times \nabla \times \underline{\underline{H}} - k^2 \underline{\underline{H}} = \nabla \times \underline{\underline{J}}_i \quad (1)$$

$$\nabla \times \nabla \times \underline{\underline{G}} - k^2 \underline{\underline{G}} = \underline{\underline{u}} \delta(\underline{\underline{r}} - \underline{\underline{r}}') \quad (2)$$

where  $\underline{\underline{J}}_i$  is the current source for the incident field and  $\underline{\underline{u}}$  is the unit dyadic. The Green's function  $\underline{\underline{G}}$  is assumed to satisfy

$$\underline{\underline{n}} \times \text{curl } \underline{\underline{G}} = 0 \quad \text{on the plates} \quad (3)$$

If we apply the vector Green's theorem for the pair (1) and (2) we obtain

$$\begin{aligned} & \int [\underline{\underline{H}}(\underline{\underline{r}}') \cdot \nabla' \times \nabla' \times \underline{\underline{G}}(\underline{\underline{r}}'; \underline{\underline{r}}) - \nabla' \times \nabla' \times \underline{\underline{H}}(\underline{\underline{r}}') \cdot \underline{\underline{G}}(\underline{\underline{r}}'; \underline{\underline{r}})] dV' \\ & = \oint_S [(\underline{\underline{n}}' \times \underline{\underline{H}}(\underline{\underline{r}}')) \cdot \text{curl } \underline{\underline{G}}(\underline{\underline{r}}'; \underline{\underline{r}}) + (\underline{\underline{n}}' \times \text{curl } \underline{\underline{H}}(\underline{\underline{r}}')) \cdot \underline{\underline{G}}(\underline{\underline{r}}'; \underline{\underline{r}})] dS' \end{aligned} \quad (4)$$

where  $S = S_1 + S_2 + S_3 + S_4 + S_B$  as indicated in figure 1. We first note that  $(\underline{\underline{n}}' \times \underline{\underline{H}}) \cdot \text{curl } \underline{\underline{G}} = -\underline{\underline{H}} \cdot (\underline{\underline{n}}' \times \text{curl } \underline{\underline{G}})$ . We also recall that  $\underline{\underline{n}}' \times \text{curl } \underline{\underline{H}} = 0$  on a perfect conductor. Using these facts and (1), (2) and (3), (4) can be rewritten as

$$\begin{aligned} \underline{\underline{H}}(\underline{\underline{r}}) - \underline{\underline{H}}_i(\underline{\underline{r}}) & = \int_{S_3+S_4} [(\underline{\underline{n}}' \times \underline{\underline{H}}) \cdot \text{curl } \underline{\underline{G}} + (\underline{\underline{n}}' \times \text{curl } \underline{\underline{H}}) \cdot \underline{\underline{G}}] dS' \\ & + \int_{S_B} (\underline{\underline{n}}' \times \underline{\underline{H}}) \cdot \text{curl } \underline{\underline{G}} dS' \end{aligned} \quad (5)$$

where

$$\underline{H}_i(\underline{r}) = \int_{V_0} \nabla' \times \underline{J}_i \cdot \underline{G} dV'$$

The integral over  $S_3 + S_4$  vanishes due to the radiation condition and (5) reduces to

$$\underline{H}(\underline{r}) = \underline{H}_i(\underline{r}) + \int_{S_B} [\underline{n}' \times \underline{H}(\underline{r}')] \cdot \text{curl } \underline{G}(\underline{r}'; \underline{r}) dS' \quad (6)$$

We can now remove the source  $\underline{J}_i$  to infinity to obtain a monochromatic plane wave as our incident field with the  $\underline{H}_i$  field parallel to the plates. Equation (6) can be converted to an integral equation for the current density  $\underline{K}(\underline{r}) = \underline{n} \times \underline{H}(\underline{r})$  in the usual manner by letting  $\underline{r}$  approach the surface of the body.

In this note we are interested in some field quantities which do not require a detailed knowledge of  $\underline{K}(\underline{r})$ . Our conducting body is a sphere of radius  $b$  (Fig. 2); we want to calculate the electric field or equivalently the charge density on the north and south pole and also the total current. These quantities only depend on the  $\phi$  independent component of the current density  $\underline{K}(\underline{r})$  and consequently we will seek a formulation for this component.  $\underline{K}(\theta)$  is directed along the  $\theta$  direction and it only depends on the  $\phi$  independent component of the incident magnetic field  $\underline{H}_i = -H_0 e^{ikx} \underline{e}_y$ . The  $\phi$  independent magnetic field has a  $\phi$  component only and satisfies the following equation

$$\frac{1}{r} \frac{\partial^2}{\partial r^2} (r H_\phi) + \frac{1}{r^2} \frac{\partial}{\partial \theta} \left[ \frac{1}{\sin \theta} \frac{\partial}{\partial \theta} (\sin \theta H_\phi) \right] + k^2 H_\phi = 0$$

(7)

or

$$(L + k^2) H_\phi = 0,$$

where the meaning of  $L$  is obvious. We first notice that

$$L = \nabla^2 - \frac{1}{r^2 \sin^2 \theta} - \frac{1}{r^2 \sin^2 \theta} \frac{\partial^2}{\partial \phi^2} \quad (8)$$

where  $\nabla^2$  is the Laplacian operator. In view of (8) we understand that  $u = H_\phi e^{i\phi}$  satisfies the scalar Helmholtz equation

$$(\nabla^2 + k^2)u = 0 \quad (9)$$

Next we introduce a Green's function  $G_1$  satisfying

$$(\nabla^2 + k^2)G_1 = -\delta(\underline{r} - \underline{r}') \quad (10)$$

with a boundary condition

$$\frac{\partial G_1}{\partial z} = 0 \quad \text{on the plates} \quad (11)$$

Applying Green's theorem for the pair (9) and (10) we arrive as before at the following equation

$$u(\underline{r}) = u_i(\underline{r}) + \int_{S_1+S_2} \left( u \frac{\partial G_1}{\partial z'} - G_1 \frac{\partial u}{\partial z'} \right) dS' + \int_{S_B} \left( u \frac{\partial G_1}{\partial r'} - G_1 \frac{\partial u}{\partial r'} \right) dS' \quad (12)$$

From Maxwell's equation  $-i\omega\epsilon_0 \underline{E} = \nabla \times \underline{H}$ , the  $\phi$  independent components  $E_\rho$  and  $H_\phi$  (where  $\rho$  is the polar radius in a suitable cylindrical coordinate system) satisfy  $i\omega\epsilon_0 E_\rho = (\partial H_\phi / \partial z)$  and consequently

$$\frac{\partial H_\phi}{\partial z} = 0 \quad \text{on the plates} \quad (13)$$

If we express  $-i\omega\epsilon_0 \underline{E} = \nabla \times \underline{H}$  in spherical coordinates we find  $i\omega\epsilon_0 r E_\theta = (\partial / \partial r)(r H_\phi)$ , i.e.,

$$\frac{\partial}{\partial r} (r H_\phi) = 0 \quad \text{on the sphere} \quad (14)$$

In view of the boundary conditions satisfied by the field  $\underline{H}$  and  $G_1$  (12) can be rewritten as

$$u(\underline{r}) = u_i(\underline{r}) + \int_{S_B} u(\underline{r}') \frac{1}{r'} \frac{\partial}{\partial r'} (r' G_1) \Big|_{r'=b} dS' \quad (15)$$

where  $dS' = b^2 \sin \theta' d\theta' d\phi'$ . The  $\phi$  independent  $\phi$  component of the incident magnetic field  $-H_0 \frac{e}{y} e^{ikx}$  is

$$\frac{1}{2\pi} (-H_0) \int_0^{2\pi} (\frac{e}{y} \cdot \frac{e}{\phi}) e^{ikr \sin \theta \cos \phi} d\phi = -iH_0 J_1(kr \sin \theta).$$

Multiplying now both sides of (15) by  $(1/2\pi)e^{-i\phi}$  and integrating from 0 to  $2\pi$  with respect to  $\phi$  we obtain

$$H_\phi(r, \theta) = -iH_0 J_1(kr \sin \theta) + \frac{1}{2\pi} \int_0^\pi d\theta' H_\phi(b, \theta') b \sin \theta' \left\{ \frac{\partial}{\partial r'} \left[ r' \int_0^{2\pi} d\phi' \int_0^{2\pi} d\phi e^{i(\phi' - \phi)} G_1(r', \theta', \phi'; r, \theta, \phi) \right] \right\}_{r'=b} \quad (16)$$

The Green's function  $G_1$  is an even function of  $\phi' - \phi$  and consequently

$$\int_0^{2\pi} d\phi \int_0^{2\pi} d\phi' G_1(|\phi - \phi'|) e^{i(\phi' - \phi)} = 2\pi \int_0^{2\pi} d\psi G_1(\psi) e^{i\psi} = 2\pi \int_0^{2\pi} d\psi \cos \psi G_1(\psi).$$

Equation (16) now reduces to

$$H_\phi(r, \theta) = -iH_0 J_1(kr \sin \theta) + \int_0^\pi H_\phi(b, \theta') \left[ \frac{\partial}{\partial r'} (r' G) \right]_{r'=b} b \sin \theta' d\theta' \quad (17)$$

where

$$G = \int_0^{2\pi} d\psi \cos \psi G_1(r, \theta, r', \theta', \psi) \quad (18)$$

We now bring  $r$  onto the surface of the sphere and (17) is converted in the usual manner into an integral equation for  $K_\theta = -H_\phi(b, \theta)$ .

$$\frac{1}{2} K_\theta(\theta) + \int_0^\pi M(\theta; \theta') K_\theta(\theta') d\theta' = iJ_1(kb \sin \theta) H_0 \quad (19)$$

with

$$M(\theta; \theta') = -b \sin \theta' \left[ \frac{\partial}{\partial r'} (r' G_1) \right]_{r'=b} \quad (20)$$

and  $G$  is given by (18) with  $r = b$ . The Green's function  $G_1$  can be computed by the method of images and is given by

$$G_1(b, \theta, r', \theta', \psi) = \sum_{m=-\infty}^{\infty} \frac{e^{-ikR_{1m}}}{4\pi R_{1m}} + \sum_{m=0}^{\infty} \left( \frac{e^{-ikR_{2m}}}{4\pi R_{2m}} + \frac{e^{-ikR_{3m}}}{4\pi R_{3m}} \right) \quad (21)$$

with

$$\begin{aligned} R_{1m} &= \left[ (2ms + z' - z)^2 + \rho^2 + \rho'^2 - 2\rho\rho' \cos \psi \right]^{\frac{1}{2}} \\ R_{2m} &= \left[ (2ms + 2h_1 - z' - z)^2 + \rho^2 + \rho'^2 - 2\rho\rho' \cos \psi \right]^{\frac{1}{2}} \\ R_{3m} &= \left[ (2ms + 2h_2 + z' + z)^2 + \rho^2 + \rho'^2 - 2\rho\rho' \cos \psi \right]^{\frac{1}{2}} \end{aligned} \quad (22)$$

where  $z = b \cos \theta$ ,  $z' = r' \cos \theta'$ ,  $\rho = b \sin \theta$ ,  $\rho' = b \sin \theta'$ ,  $h_1 + h_2 = s$ . The current  $I(\theta)$  is given by

$$I(\theta) = \int_0^{2\pi} K_\theta(\theta, \phi) b \sin \theta d\phi.$$

If we expand  $K_\theta(\theta, \phi)$  in a Fourier series, then we see that  $I(\theta)$  only depends on the  $\phi$  independent component of  $K_\theta(\theta, \phi)$ . Thus,

$$I(\theta) = 2\pi b \sin \theta K_\theta(\theta) \quad (23)$$

The current density  $\sigma$  at a given point  $(\theta, \phi)$  does depend on  $\phi$ . For  $\theta = 0, \pi$  we should obtain the same value for  $\sigma$  no matter what  $\phi$  is, and  $\sigma$  cannot depend on  $\phi$  at these two points. Thus,  $\sigma$  at  $\theta = 0, \pi$  coincides with the  $\phi$  independent component of the charge density. It can be obtained through the continuity equation

$$i\omega\sigma = \frac{1}{b \sin \theta} \frac{\partial}{\partial \theta} (\sin \theta K_\theta) \quad (24)$$

where  $K_\theta$  and  $\sigma$  are the  $\phi$  independent current density and charge density respectively. First we calculate  $\sigma$  at  $\theta = 0$ . We rewrite (24) as

$$i\omega\sigma = \frac{1}{b} \frac{\partial K_\theta}{\partial \theta} + \frac{\cos \theta}{\sin \theta} K_\theta.$$

As  $\theta \rightarrow 0$ ,

$$\frac{\cos \theta}{\sin \theta} K_\theta \rightarrow \left. \frac{\partial K_\theta}{\partial \theta} \right|_{\theta=0}$$

and (24) becomes

$$\sigma = - \left. \frac{2i}{\omega b} \frac{\partial K_\theta}{\partial \theta} \right|_{\theta=0} \quad (25)$$

$K_\theta$  is zero at  $\theta = 0$ , therefore,

$$\left. \frac{\partial K_\theta}{\partial \theta} \right|_{\theta=0} = \left. \frac{K_\theta}{\theta} \right|_{\theta=0}$$

or

$$\sigma = - \left. \frac{2i}{\omega b} \frac{K_\theta}{\theta} \right|_{\theta=0} \quad (26)$$

From the numerical computation point of view (25) or (26) cannot give accurate results unless (19) is numerically integrated using a large number of zones. We can improve the accuracy by calculating  $\sigma$  as an integral over  $K_\theta$ . If we combine (19) and (25) we obtain

$$\sigma = 2 \frac{H_0}{c} + \int_0^\pi N(\theta') K_\theta(\theta') d\theta' \quad (27)$$

where

$$N(\theta') = - \left. \frac{4i}{\omega b} \left[ \frac{\partial}{\partial \theta} M(\theta, \theta') \right] \right|_{\theta=0} \quad (28)$$

Noticing that  $H_0/E_0 = (\epsilon_0/\mu_0)^{1/2}$ , i.e.  $H_0/c = \epsilon_0 E_0$  (27) becomes

$$\sigma(\theta=0) = 2\epsilon_0 E_0 + \int_0^\pi N(\theta') K_\theta(\theta') d\theta' \quad (29)$$

For a given accuracy of  $K_\theta$  the charge density  $\sigma(\theta=0)$  calculated through (29) is more accurate than  $\sigma$  given by (26). To calculate  $\sigma(\theta=\pi)$  we use (29) with the  $\theta$  dependence of  $K_\theta$  reversed. The result is equal to  $-\sigma(\theta=\pi)$ .

In this note we will consider the case of one plate only (Fig. 3), and in a future note we will study the two-plate problem. The formulation is still the same except that  $G_1$  is considerably simplified. Instead of (21) we now have

$$G_1(b, \theta, r', \theta', \psi) = \frac{e}{4\pi R_{10}} + \frac{e}{4\pi R_{30}} \quad (30)$$

where

$$\begin{aligned} R_{10} &= \left[ (z - z')^2 + \rho^2 + \rho'^2 - 2\rho\rho' \cos \psi \right]^{\frac{1}{2}} \\ R_{30} &= \left[ (2h_2 + z' + z)^2 + \rho^2 + \rho'^2 - 2\rho\rho' \cos \psi \right]^{\frac{1}{2}} \end{aligned} \quad (31)$$

$$z = b \cos \theta, \quad z' = r' \cos \theta', \quad \rho = b \sin \theta, \quad \rho' = r' \sin \theta'.$$

When  $r' = b$ ,  $\theta = \theta'$  then  $R_{10} = 0$ , and the Kernel in (17) is singular. This is an integrable singularity and in the Appendix we show how to treat this singularity in order to perform the integration numerically on a computer.

### III. Low, High-Frequency and Late, Early-Time Behavior

For a plane wave of low frequency the wavelength is much larger than the radius of the sphere and we have a quasi-static situation. Consider now a step pulse illuminating the sphere. At late times the pulse has well enveloped the sphere and the induced charges have again settled to a quasi-static state. Thus, we expect the current and charge densities to asymptotically reach their static values at late times. This value is zero for the current. For a plane wave of high frequency the wavelength is much smaller than the radius of the sphere and the interaction has a local character. The current density and charge density are  $2\underline{n} \times \underline{H}^{inc}$  and  $2\underline{n} \cdot \underline{E}^{inc}$  in the illuminated region and zero in the shadow region. We are interested in the values of the charge density at  $\theta = 0$  and  $\pi$ , i.e., right on the shadow boundary. Fock (Ref. 10) and others (see for example Ref. 11) have worked out the values of the current density in the transition region. They have found that in this region,  $\underline{K}(\theta, \phi) = \underline{K}^{inc}(\theta, \phi)G(\xi)$  where  $\xi$  is negative in the illuminated region and positive in the shadow region. At  $\xi = 0$ , i.e., on the shadow boundary  $G(\xi) = 1.3990$  whereas for  $\xi$  large and negative ( $|\xi| > 3$ )  $G(\xi) \approx 2$  and for  $\xi$  large and positive ( $\xi > 5$ )  $G(\xi) \approx 0$ . In view of (26) the same considerations are valid for the charge density at  $\theta = 0$  and also  $\theta = \pi$ . Thus, the value of  $\sigma(\theta=0, \pi)$  is  $1.3990 \epsilon_0 E_0$  as  $kb \rightarrow \infty$ . Consider now a step pulse incident upon the sphere. As the front comes in contact with the sphere the interaction has local character. Thus, the charge density at the poles (at  $t = 0+$ ) should assume the high frequency value  $1.3990 \epsilon_0 E_0$ . Notice that the presence of the plates does not change this value. The total current varies as  $k^{-1/2}$  and goes to zero for either  $kb \rightarrow \infty$  or  $t = 0+$ . This can be seen by examining (19).

#### IV. Discussion of Plots

We present plots of the charge densities at the poles and the equator current. The pole closest to the ground plate is designated as B (bottom) and the other pole as T (top). We normalize the charge densities either dividing them by  $\epsilon_0 E_0$  or by the appropriate free space value. The equator current is denoted as I and the normalizing factor is either  $bH_0$  or the free space value. Thus, we give the following plots

- Figure 7  $\sigma_B(t)/\epsilon_0 E_0$  versus  $ct/b$   
 Figure 8  $|\sigma_B(\omega)|/\epsilon_0 E_0$  versus  $kb$   
 Figure 9,10  $|\sigma_B(\omega)|/\epsilon_0 E_0$  versus  $kb$ , expanded scale  
 Figure 11  $\sigma_T(t)/\epsilon_0 E_0$  versus  $ct/b$   
 Figure 12  $|\sigma_T(\omega)|/\epsilon_0 E_0$  versus  $kb$   
 Figure 13  $I(t)/bH_0$  versus  $ct/b$   
 Figure 14  $|I(\omega)|/bH_0$  versus  $kb$   
 Figure 15  $\max \sigma_B(t)/\epsilon_0 E_0$  versus  $\delta/b$  where  $\max \sigma_B(t)$  is the maximum value attained by  $\sigma_B(t)$  in the time domain  
 Figure 16  $C_m(B)$  versus  $\delta/b$  where  $C_m(B)$  is the ratio of the maximum  $\sigma_B(t)$  for a given  $\delta/b$  to the maximum  $\sigma_B(t)$  for  $\delta/b = \infty$  (free space)  
 Figure 17  $\max |\sigma_B(\omega)|/\epsilon_0 E_0$  versus  $\delta/b$  where  $\max |\sigma_B(\omega)|$  is the maximum value of  $|\sigma_B(\omega)|$  corresponding to the first resonance  
 Figure 18  $C_r(B)$  versus  $\delta/b$  where  $C_r(B)$  is the ratio of the maximum  $|\sigma_B(\omega)|$  for a given  $\delta/b$  to the maximum  $|\sigma_B(\omega)|$  for  $\delta/b = \infty$  (free space)  
 Figure 19  $\sigma_B(\omega = 0)/\epsilon_0 E_0$  versus  $\delta/b$  where  $\sigma_B(\omega = 0)$  is the static value at B  
 Figure 20  $C_s(B)$  versus  $\delta/b$  where  $C_s(B)$  is the ratio of the static value of  $\sigma_B$  for a given  $\delta/b$  to the static value of  $\sigma_B$  for  $\delta/b = \infty$  (free space)  
 Figure 21 through Figure 26 are the same as 15 through 20 except they refer to the charge density at T  
 Figure 27  $\max |I(\omega)|/bH_0$  versus  $\delta/b$  where  $\max |I(\omega)|$  is the value of  $|I(\omega)|$  at the first resonance  
 Figure 28  $C_r(I)$  versus  $\delta/b$  where  $C_r(I)$  is the ratio of the value of I for a given  $\delta/b$  at the first resonance to the value of I for  $\delta/b = \infty$  (free space) at the corresponding first resonance.

No plots of  $\max I(t)$  versus  $\delta/b$  or  $C_m(I)$  versus  $\delta/b$  are given because the percentage differences between the maximum values of  $I$  for various  $\delta/b$  are small ( $\leq 7.5\%$ ).

The zero time for the charge densities is taken as the moment of the arrival of the step pulse wavefront at the center of the sphere and the zero time for the current is the moment of contact of the wavefront with the sphere. The effect of the ground plate or equivalently of the image sphere occurs at a retarded time depending on the quantity of interest and the gap size. The computation of the retardation times are given in Appendix B. For the pole B the ray that travels the least time is the one that suffers a specular reflection at a point on the surface of the image sphere (Fig. 4 and 5). In Appendix C we give a proof that any deviation from the specular reflection path results in a longer retarded time. A direct specular reflection path is not feasible for either the points on the equator or T. For the current the least time path consists of a specular reflection off the image sphere such that the reflected ray will be tangent to the real sphere plus an arc path along the surface of the latter sphere (Fig. 6). To obtain the minimum time path for point T, at the top of the sphere, we should add an arc of  $90^\circ$  to the current path.

In the frequency domain the presence of the ground plate can have a pronounced effect on the amplitude of the charge density  $|\sigma_B(\omega)|$  but a less pronounced of the first resonant frequency. The corresponding effects on  $|\sigma_T(\omega)|$  and  $|I(\omega)|$  are much less pronounced for the amplitude but comparable for the first resonant frequency; however, the presence of the ground plane can cause some additional secondary resonances which are not present in the free space case. These resonances appear to be predominant for  $|\sigma_T(\omega)|$  and  $|I(\omega)|$  only. The reason is that additional resonances for  $|\sigma_B(\omega)|$  due to the proximity effect can only occur for large  $kb$  at which the gap can be comparable to the wavelength and at large  $kb$  the amplitude tends to settle down to the high frequency limit which is independent of the presence of the ground plate, i.e., the resonances would appear as minor perturbations. Finally, we would like to make two remarks with respect to the time response of the sphere. First, the time at which the quantity of interest (charge density or current) reaches its

peak value has only a slight dependence on the gap size. Second, the time interval from the peak to a value which has a percentage difference from the final (static) value less than 4% is short compared to a thin cylindrical structure (see for example Ref. 2) and is given by  $\Delta t \approx 10b/c$ . This last estimate refers to the charge densities since the current settles down to zero for large  $ct/b$ .

Appendix A

The kernel  $M(\theta; \theta')$  given by (20) can be rewritten as

$$M(\theta; \theta') = \int_0^{2\pi} d\psi \cos \psi M_1(\theta, \theta', \psi), \quad (\text{A-1})$$

where

$$M_1(\theta, \theta', \psi) = -b \sin \theta' \left[ G_{10} \left( \frac{1}{2} + \frac{1}{2} ikR_{10} \right) + G_{30} \left( 1 + ikb \frac{B_{30}}{R_{30}} - \frac{bB_{30}}{R_{30}^2} \right) \right] \quad (\text{A-2})$$

and

$$G_{10} = \frac{e^{ikR_{10}}}{4\pi R_{10}}, \quad G_{30} = \frac{e^{ikR_{30}}}{4\pi R_{30}}$$

$$B_{30} = b[2(h_2/b)\cos \theta' + 1 + \cos \theta \cos \theta' - \sin \theta \sin \theta' \cos \psi],$$

$$R_{10} = \sqrt{2} b(1 - \cos \theta \cos \theta' - \sin \theta \sin \theta' \cos \psi)^{\frac{1}{2}}, \quad (\text{A-3})$$

$$R_{30} = b[(2(h_2/b) + \cos \theta + \cos \theta')^2 + \sin^2 \theta + \sin^2 \theta' - 2 \sin \theta \sin \theta' \cos \psi]^{\frac{1}{2}}.$$

We understand that the only term singular at  $\theta = \theta'$ ,  $\psi = 0$  is  $-1/2 b \sin \theta' G_{10} = -1/2 b \sin \theta' (e^{ikR_{10}}/4\pi R_{10})$ . We treat this term as follows. First we define

$$M_1(\theta, \theta', \psi) = -\frac{1}{2} b \sin \theta' G_{10} + M_2(\theta, \theta', \psi) \quad (\text{A-4})$$

and rewrite (19) as

$$\begin{aligned} & \frac{1}{2} K_\theta(\theta) - \frac{1}{2} b \int_0^\pi [K_\theta(\theta') - K_\theta(\theta)] \left\{ \int_0^{2\pi} d\psi \cos \psi G_{10} \right\} \sin \theta' d\theta' \\ & - \frac{1}{2} b K_\theta(\theta) \int_0^\pi d\theta' \sin \theta' \int_0^{2\pi} d\psi \cos \psi G_{10} + \int_0^\pi K_\theta(\theta') \int_0^{2\pi} d\psi \cos \psi M_2(\theta, \theta', \psi) \\ & = iJ_1(kb \sin \theta) H_0 \end{aligned} \quad (\text{A-5})$$

Thus, we have to evaluate

$$I = \int_0^\pi d\theta' \sin \theta' \int_0^{2\pi} d\psi \cos \psi G_{10} \quad (\text{A-6})$$

separately. Define

$$I_1 = \int_0^{2\pi} d\psi \cos \psi G_{10} = 2 \int_0^\pi d\psi \cos \psi \frac{e^{ikR_{10}}}{4\pi R_{10}} \quad (\text{A-7})$$

and

$$A = (1 - \cos \theta \cos \theta')^{\frac{1}{2}} \quad (\text{A-8})$$

$$B = \frac{\sin \theta \sin \theta'}{1 - \cos \theta \cos \theta'}$$

Thus,

$$I_1 = \frac{1}{2(2)^{\frac{1}{2}}\pi A} \int_0^\pi d\psi \frac{\cos \psi e^{ikR_{10}}}{(1-B \cos \psi)^{\frac{1}{2}}} = \frac{1}{2(2)^{\frac{1}{2}}\pi A} I_2 \quad (\text{A-9})$$

To cast  $I_2$  into a form suitable for numerical integration on a computer we subtract the singularity at  $\theta = \theta'$  and perform the remaining integration explicitly, i.e.,

$$I_2 = \int_0^\pi \left[ \frac{\cos \psi e^{ikR_{10}}}{(1-B \cos \psi)^{\frac{1}{2}}} - \frac{1}{(1-B+(B/2)\psi^2)^{\frac{1}{2}}} \right] d\psi + \int_0^\pi \frac{d\psi}{(1-B+(B/2)\psi^2)^{\frac{1}{2}}} \quad (\text{A-10})$$

and

$$I_3 = \int_0^\pi \frac{d\psi}{(1-B+(B/2)\psi^2)^{\frac{1}{2}}} = \left(\frac{2}{B}\right)^{\frac{1}{2}} \left\{ \ln \left[ \pi \left(\frac{B}{2}\right)^{\frac{1}{2}} + \left(\frac{B\pi^2}{2} + 1 - B\right)^{\frac{1}{2}} \right] - \frac{1}{2} \ln(1 - B) \right\} \quad (\text{A-11})$$

That last term in (A-10) is singular and to perform the  $\theta'$  integration we have to subtract this singularity out. Following a similar procedure as before we finally arrive at the integral equation

$$\begin{aligned}
& \frac{1}{8\pi} K_{\theta}(\theta) \left\{ 4\pi + \int_0^{\pi} \left\{ \ln \left[ 1 - \cos(\theta - \theta') \right] - \ln \frac{(\theta - \theta')^2}{2} \right\} d\theta' \right. \\
& - \int_0^{\pi} \left[ \ln(1 - \cos \theta \cos \theta') - \ln \frac{\theta^2 + \theta'^2}{2} \right] d\theta' \\
& \left. - \pi \ln(\theta^2 + \pi^2) - 2\theta \tan^{-1} \frac{\pi}{\theta} + 2\theta \ln \theta + 2(\pi - \theta) \ln(\pi - \theta) \right\} \\
& + \frac{1}{8\pi} \int_0^{\pi} \left[ K_{\theta}(\theta') - K_{\theta}(\theta) \right] \ln(1 - B(\theta, \theta')) d\theta' \\
& + 2 \int_0^{\pi} d\theta' K_{\theta}(\theta') \int_0^{\pi} d\psi \cos \psi M_2(\theta, \theta', \psi) = iJ_1(kb \sin \theta) H_0 \tag{A-12}
\end{aligned}$$

where  $M_2(\theta, \theta', \psi)$  has been defined in (A-4). All the integrals involved in (A-12) have nonsingular integrands and they are suitable for numerical integration on a computer.

## Appendix B

### 1. Retardation time for $\sigma_B$

Referring to Fig. 5 we can easily establish the relationships

$$\psi = 2\beta - \pi/2 \quad (B-1)$$

$$(1B)\cos \psi + b \sin \beta = b + 2\delta \quad (B-2)$$

$$(1B)\sin \psi = b \cos \beta \quad (B-3)$$

In view of (B-1), (B-2) and (B-3) can be rewritten as

$$(1B)\sin 2\beta + b \sin \beta = b + 2\delta \quad (B-4)$$

$$- (1B)\cos 2\beta = b \cos \beta \quad (B-5)$$

Combining (B-4) and (B-5) we can derive the following relationships

$$\sin \beta = \frac{1 + \sqrt{1 + 8(1 + 2\delta/b)^2}}{4(1 + 2\delta/b)} \quad (B-6)$$

$$(1B)/b = \left[ 1 + (1 + 2\delta/b)^2 - 2(1 + 2\delta/b)\sin \beta \right]^{1/2} \quad (B-7)$$

Recalling that the zero time for the charge density at B is taken as the moment of arrival of the wavefront at the center of the sphere we understand that the normalized retardation time is

$$\begin{aligned} \frac{cT(B)}{b} &= \frac{(1B) - (12)}{b} = \frac{(1B)}{b} (1 + \cos 2\beta) = \frac{(1B)}{b} \cos^2 \beta \\ &= \left( 1 - \frac{\sin \beta}{1 + 2\delta/b} \right) \left[ 1 + (1 + 2\delta/b)^2 - 2(1 + 2\delta/b)\sin \beta \right]^{1/2} \end{aligned}$$

The angle  $\beta$  as given by (B-6) ranges from  $90^\circ$  ( $\delta/b = 0$ ) to  $45^\circ$  ( $\delta/b = \infty$ ).

2. Retardation times for I and  $\sigma_T$

Referring to Fig. 6 we can easily establish the following relationships

$$\psi = \pi/2 - 2\beta \quad (B-8)$$

$$b \sin \psi + (23)\cos \psi + b \sin \beta = 2b + 2\delta \quad (B-9)$$

$$b \cos \psi = (23)\sin \psi + b \cos \beta \quad (B-10)$$

In view of (B-8), (B-9) and (B-10) can be rewritten as

$$b \cos 2\beta + (23)\sin 2\beta + b \sin \beta = 2b + 2\delta \quad (B-11)$$

$$b \sin 2\beta = (23)\cos 2\beta + b \cos \beta \quad (B-12)$$

Combining (B-11) and (B-12) we can derive the following relationships

$$\sin \beta = \frac{1 + \sqrt{1 + 16(1 + \delta/b)(1 + 2\delta/b)}}{8(1 + 2\delta/b)} \quad (B-13)$$

$$\frac{(23)}{b} = 2\{[1 + (\delta/b)^2] - (1 + \delta/b)\sin \beta\}^{\frac{1}{2}} \quad (B-14)$$

Recalling that the zero time for the current is taken as the moment of arrival of the wavefront at point 4 the normalized retardation time is given by

$$\frac{CT(I)}{b} = \psi + \frac{(12)+(23)}{b} = \psi + (1 - \cos \beta) + \frac{(23)}{b}$$

where  $\psi = \pi/2 - 2\beta$ ,  $\beta$  is given by (B-13) and  $(23)/b$  by (B-14). The angle  $\beta$  ranges from  $39.821^\circ$  for  $\delta/b = 0$  to  $45^\circ$  for  $\delta/b = \infty$ .

The retardation time for point T, at the top of the sphere, is

$$\frac{cT(T)}{b} = \frac{c}{b} T(I) + \pi/2 - 1$$

We have added  $\pi/2$  to take into consideration the additional path of  $90^\circ$  and subtracted unity to account for the fact that the zero time for the charge density at point T is the instant of arrival of the wavefront at the center of the sphere.

### Appendix C

The specular reflection path is the least time path. Consider an alternate path which deviates from the specular reflection path by an angle  $\Delta\beta$  (Fig. 4). We want to compare (1B) to (1B) + (2B). We can easily derive the relationships

$$(1B)^2 = b^2 + (2\delta + b)^2 - 2b(2\delta + b)\sin \beta \quad (C-1)$$

$$(2B)^2 = b^2 + (2\delta + b)^2 - 2b(2\delta + b)\sin(\beta + \Delta\beta) \quad (C-2)$$

We expand  $\sin(\beta + \Delta\beta)$  and we consider terms up to order  $(\Delta\beta)^2$

$$\begin{aligned} \sin(\beta + \Delta\beta) &= \sin \beta \cos \Delta\beta + \cos \beta \sin \Delta\beta \\ &= \sin \beta + \Delta\beta \cos \beta - \frac{(\Delta\beta)^2}{2} \sin \beta + O[(\Delta\beta)^3] \end{aligned} \quad (C-3)$$

In view of (C-3) and (C-1) we can rewrite (C-2) as follows

$$(2B)^2 = (1B)^2 - 2b(2\delta + b)\Delta\beta \cos \beta + b(2\delta + b)\sin \beta(\Delta\beta)^2 + O[(\Delta\beta)^3]$$

or

$$(2B) = (1B) \left\{ 1 - \frac{2b(2\delta+b)}{(1B)^2} \cos \beta(\Delta\beta) + \frac{b(2\delta+b)}{(1B)^2} \sin \beta(\Delta\beta)^2 + O[(\Delta\beta)^3] \right\}^{\frac{1}{2}} \quad (C-4)$$

Employing the binomial expansion  $(1 + \epsilon)^{\frac{1}{2}} = 1 + (1/2)\epsilon - (1/8)\epsilon^2 + \dots$  we can rewrite (C-4) as

$$\begin{aligned} (2B) &= (1B) \left\{ 1 - \frac{b(2\delta+b)}{(1B)^2} \cos \beta(\Delta\beta) + \frac{b(2\delta+b)}{2(2B)^2} \sin \beta(\Delta\beta)^2 \right. \\ &\quad \left. - \frac{1}{8} \left[ \frac{2b(2\delta+b)}{(1B)^2} \right]^2 \cos^2 \beta(\Delta\beta)^2 + O[(\Delta\beta)^3] \right\} \end{aligned} \quad (C-5)$$

From Fig. 4 we see that

$$(12) = 2b \sin \frac{\Delta\beta}{2}$$

$$\begin{aligned} (13) &= (12)\cos \psi = 2b \sin \frac{\Delta\beta}{2} \cos(\pi/2 - \beta - \frac{\Delta\beta}{2}) \\ &= b \sin \beta (\Delta\beta) + \frac{b}{2} \cos \beta (\Delta\beta)^2 + 0[(\Delta\beta)^3] \end{aligned} \quad (C-6)$$

Combining (C-5) and (C-6) we find

$$\begin{aligned} (2B) + (13) - (1B) &= b(\Delta\beta) \left[ \sin \beta - \frac{2\delta+b}{(1B)} \cos \beta \right] \\ &+ \frac{1}{2} b(\Delta\beta)^2 \left[ \cos \beta + \frac{2\delta+b}{(1B)} \sin \beta - \frac{b(2\delta+b)^2}{(1B)^2} \cos^2 \beta \right] \\ &+ 0[(\Delta\beta)^3] \end{aligned} \quad (C-7)$$

From Fig. 4 we find that

$$(2\delta + b)\cos \beta = (4B) = (1B)\sin \beta$$

This shows that the first order term  $\Delta\beta$  is zero which is in accordance with the principle of least action. Next we examine the second order term. We notice that

$$(2\delta + b)\sin \beta = b + (14)$$

$$(2\delta + b)\cos \beta = (4B)$$

and (C-7) gives

$$(2B) + (1B) - (1B) = \frac{1}{2} b(\Delta\beta)^2 \left[ \cos \beta + \frac{(14)}{(1B)} + \frac{b}{(1B)} - \frac{b}{(1B)} \frac{(4B)^2}{(1B)^2} \right] + 0[(\Delta\beta)^3]$$

Recalling that  $\beta < \pi/2$ ,  $(4B) < (1B)$ ,  $(14) > 0$  we understand that the second order term is positive. If we choose a ray with a variation  $\Delta\beta$  in the opposite direction we can similarly show that the second order term is positive. Thus, any paths that deviate from the specular reflection path by  $\Delta\beta$  correspond to a longer time.

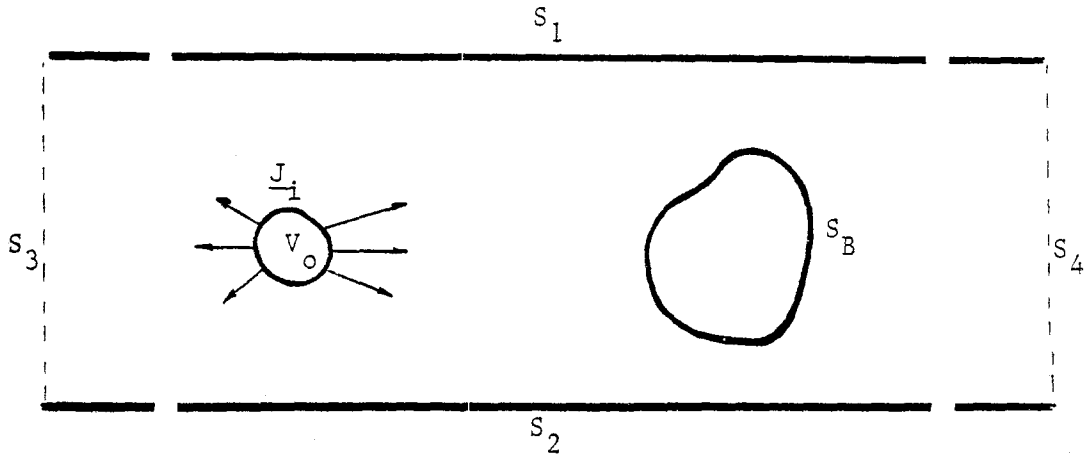


Figure 1. A metallic object within a two-parallel-plate simulator.

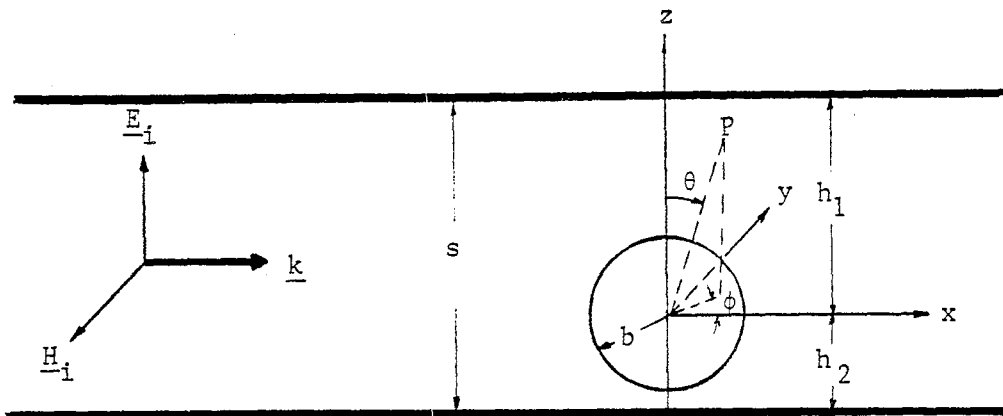


Figure 2. A metallic sphere within a two-parallel-plate simulator.

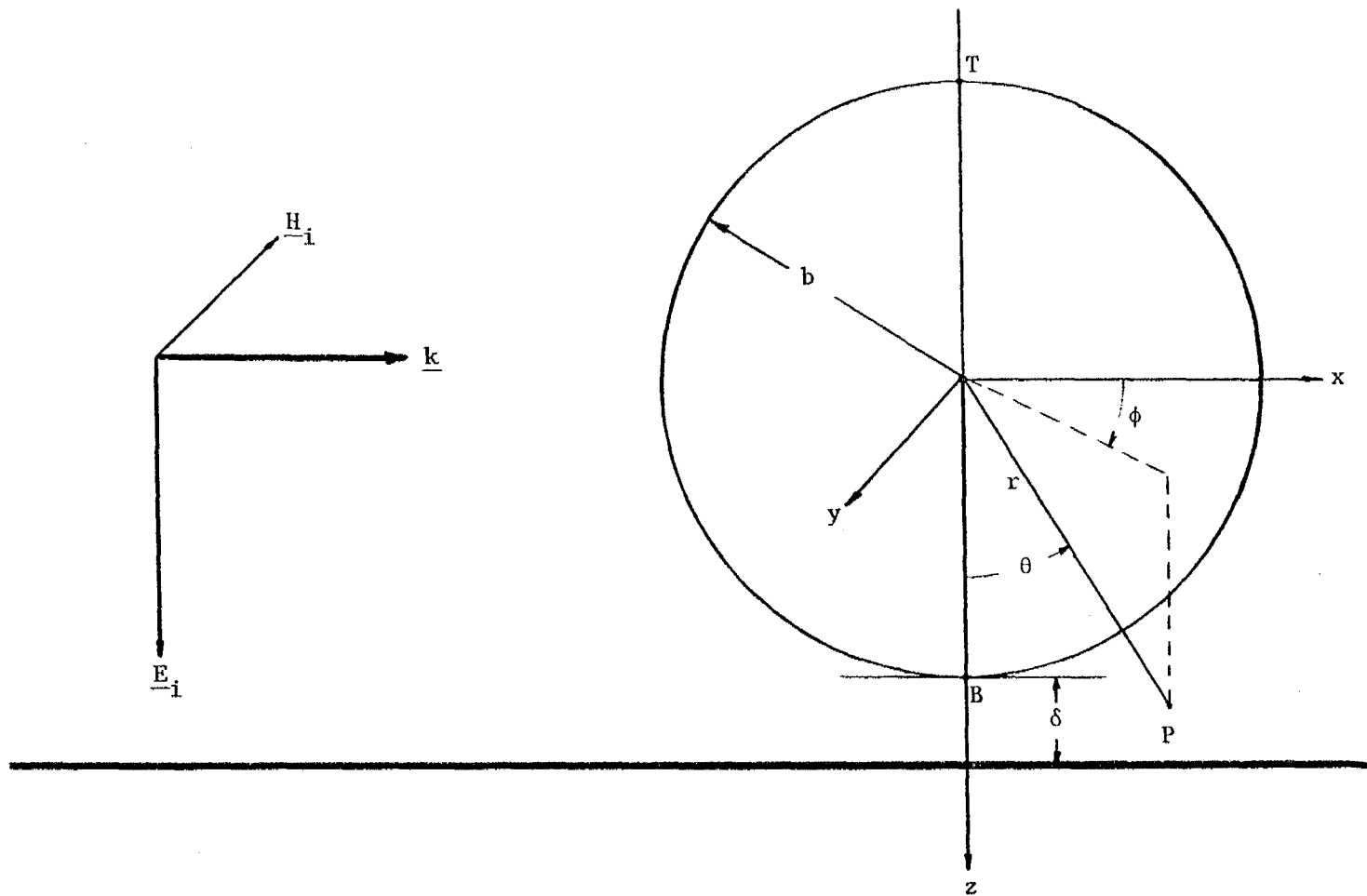


Figure 3. A metallic sphere above a ground plate illuminated by a monochromatic plane wave.

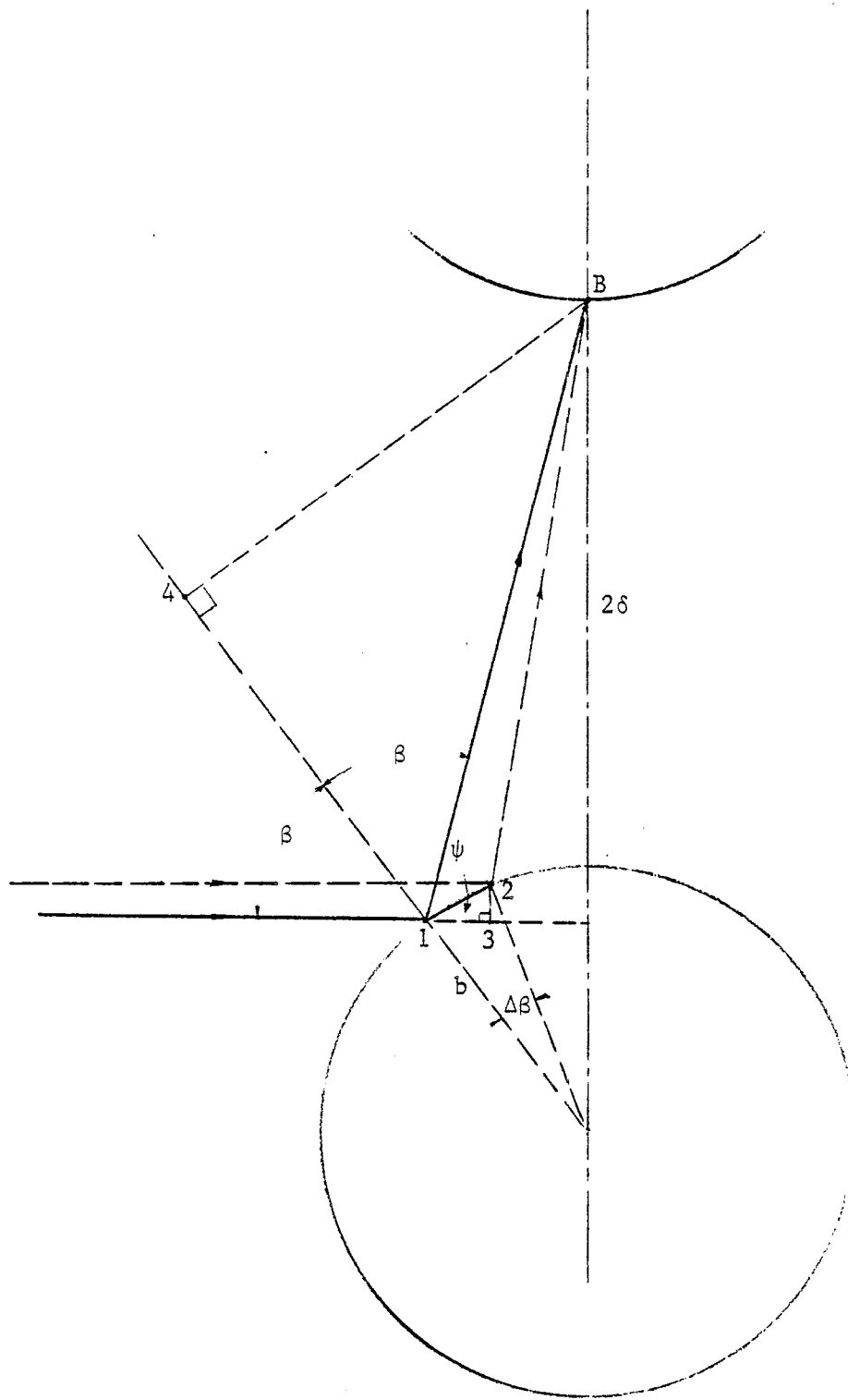


Figure 4. Geometry depicting the specular reflection path and an alternative path. The bottom pole B first senses the presence of the ground plate, or equivalently the image sphere, through the specular reflection path.

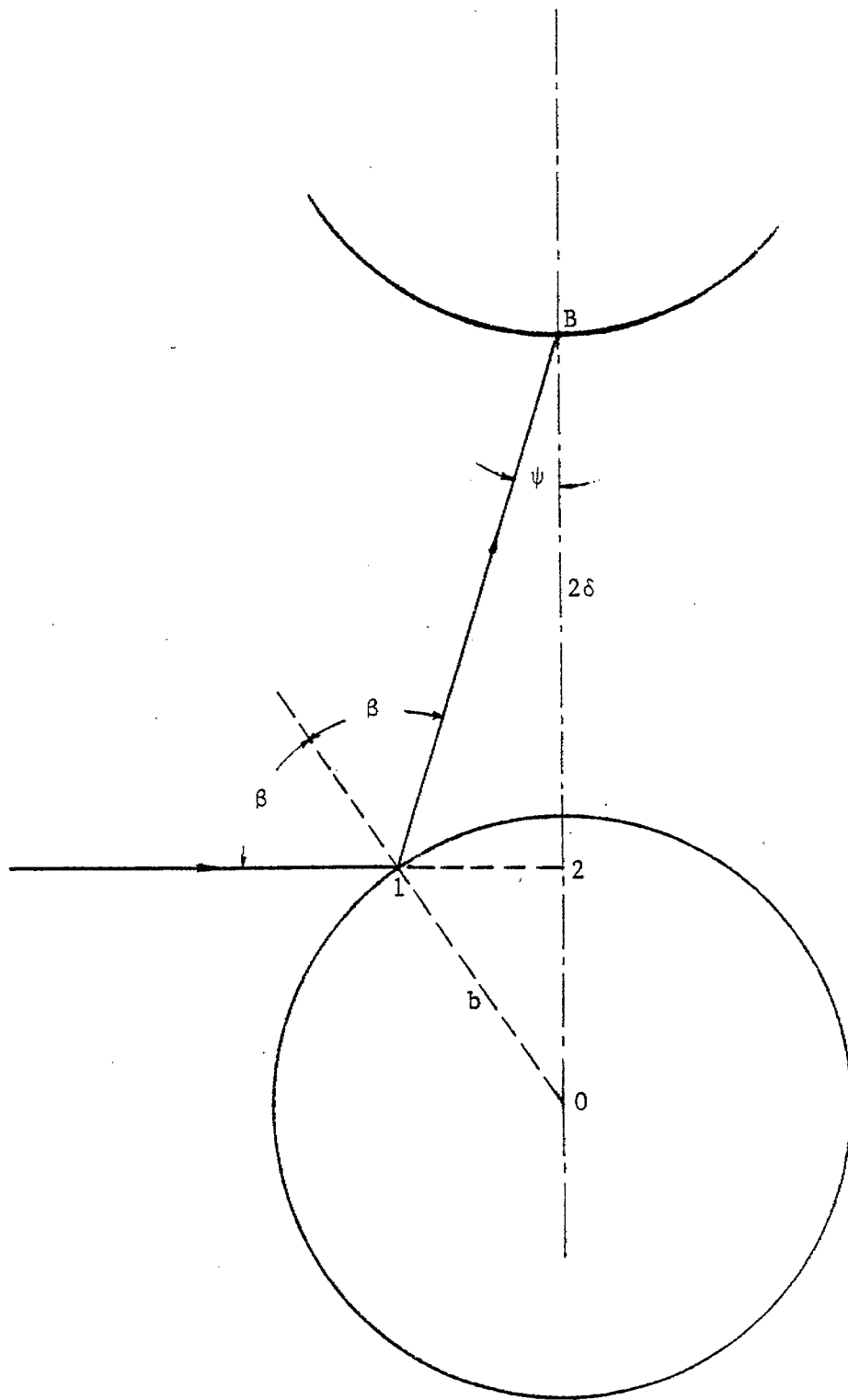


Figure 5. Geometry for the computation of the minimum time specular reflection path.

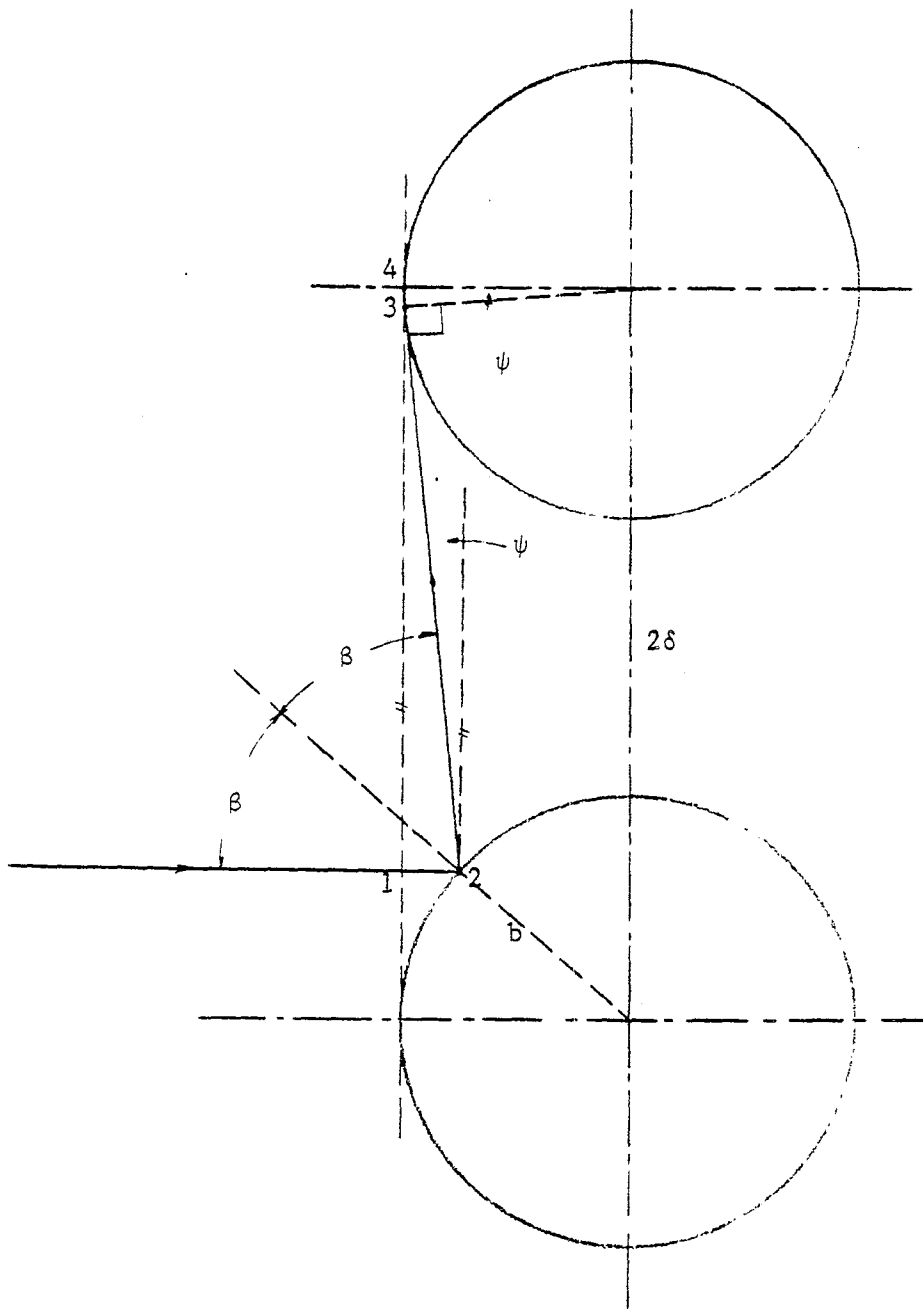


Figure 6. Geometry for the minimum time path involving the interaction of the sphere and the ground plate, or equivalently the image sphere, at the equator points. The path consists of a specular reflection off the image sphere and an arc path along the principal sphere.

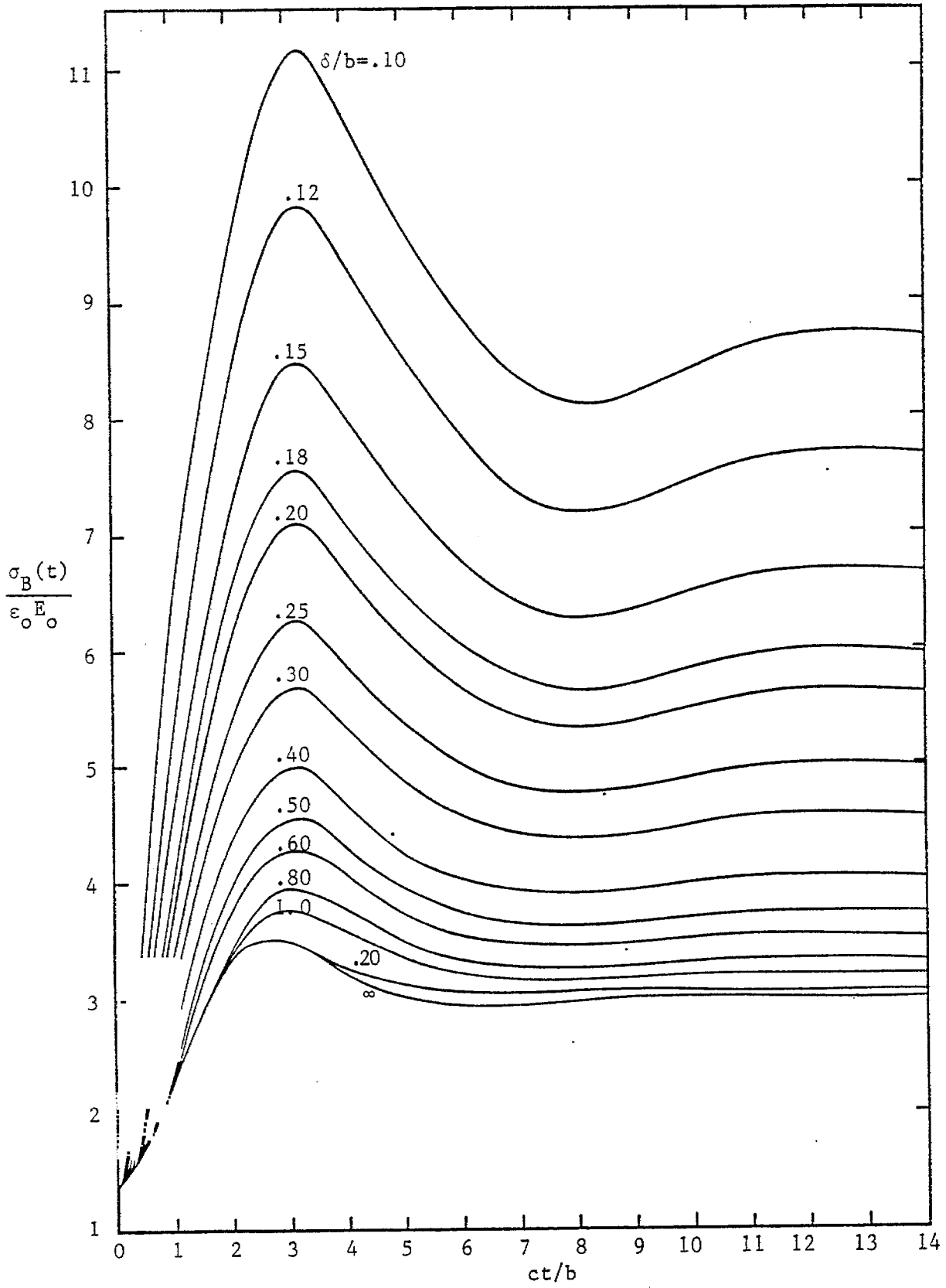


FIGURE 7

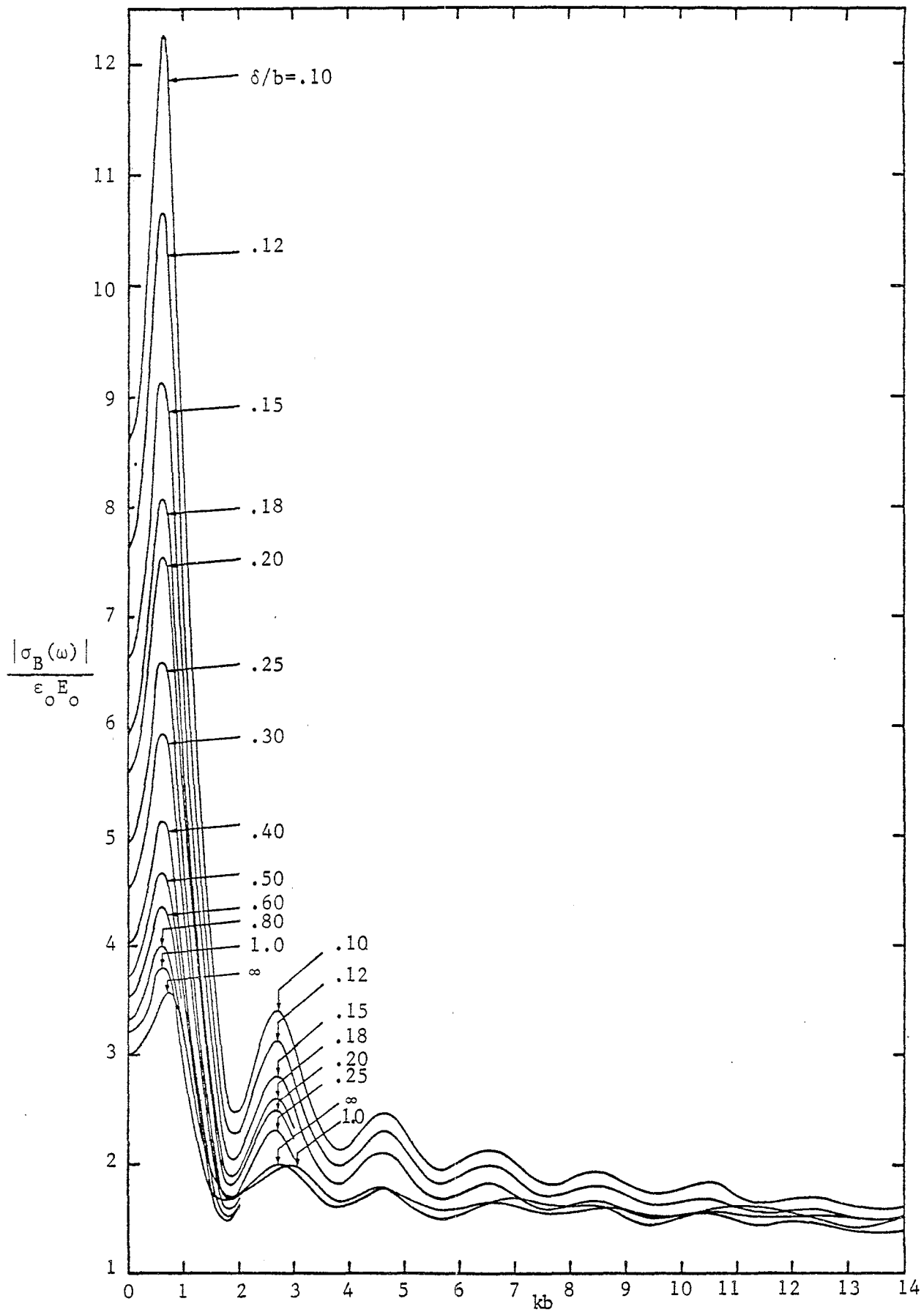


FIGURE 8

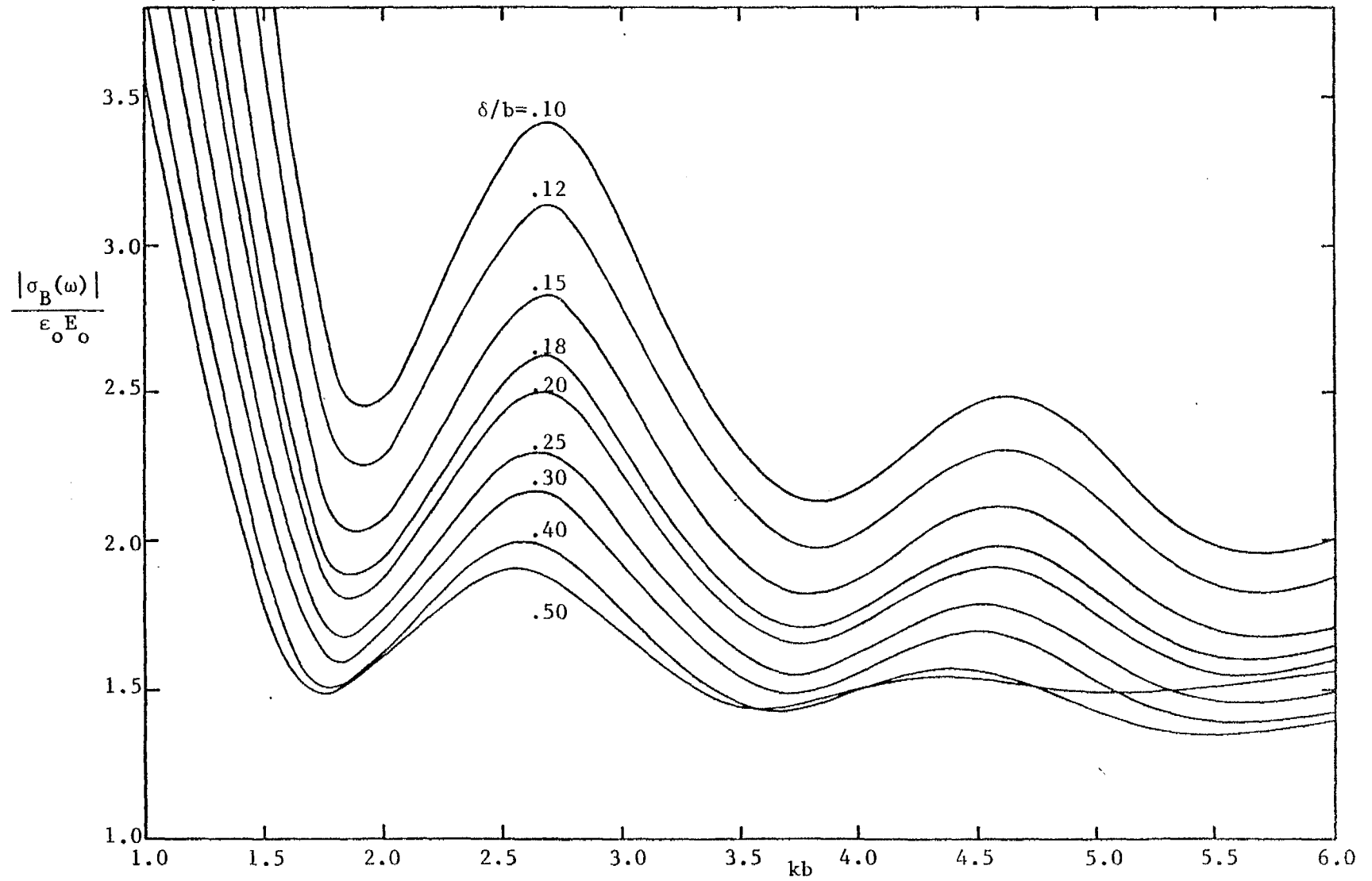


FIGURE 9

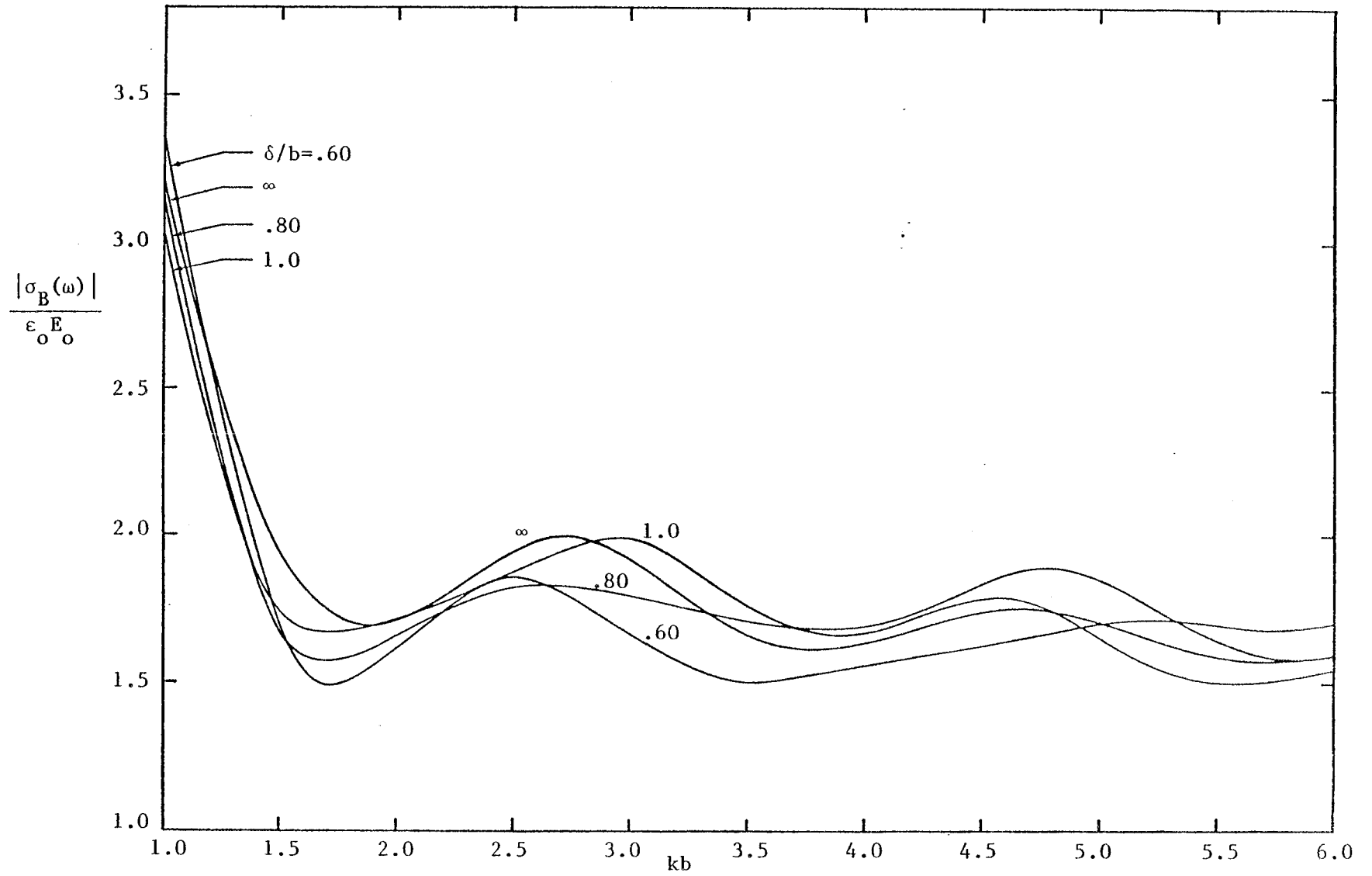


FIGURE 10

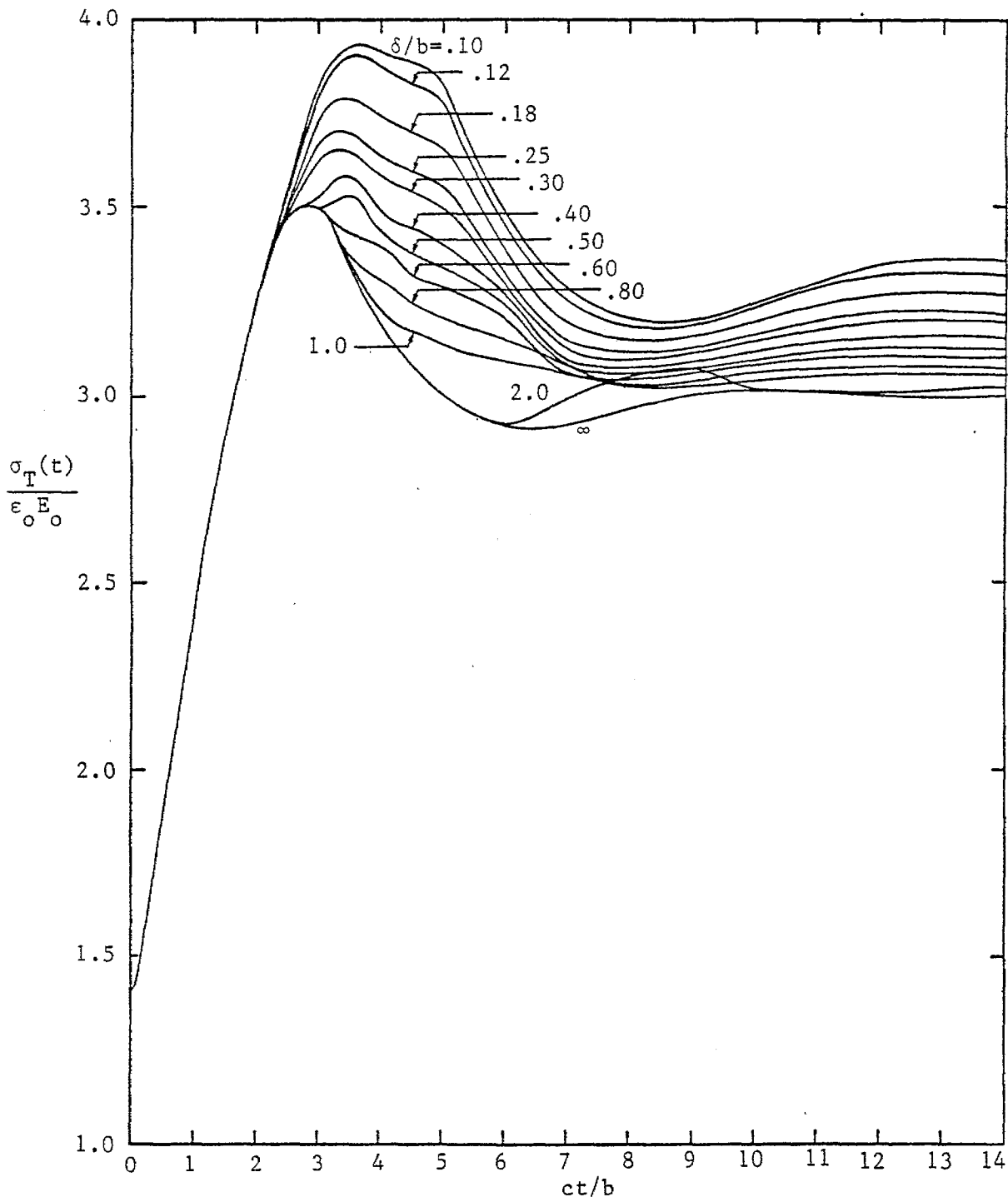


FIGURE 11

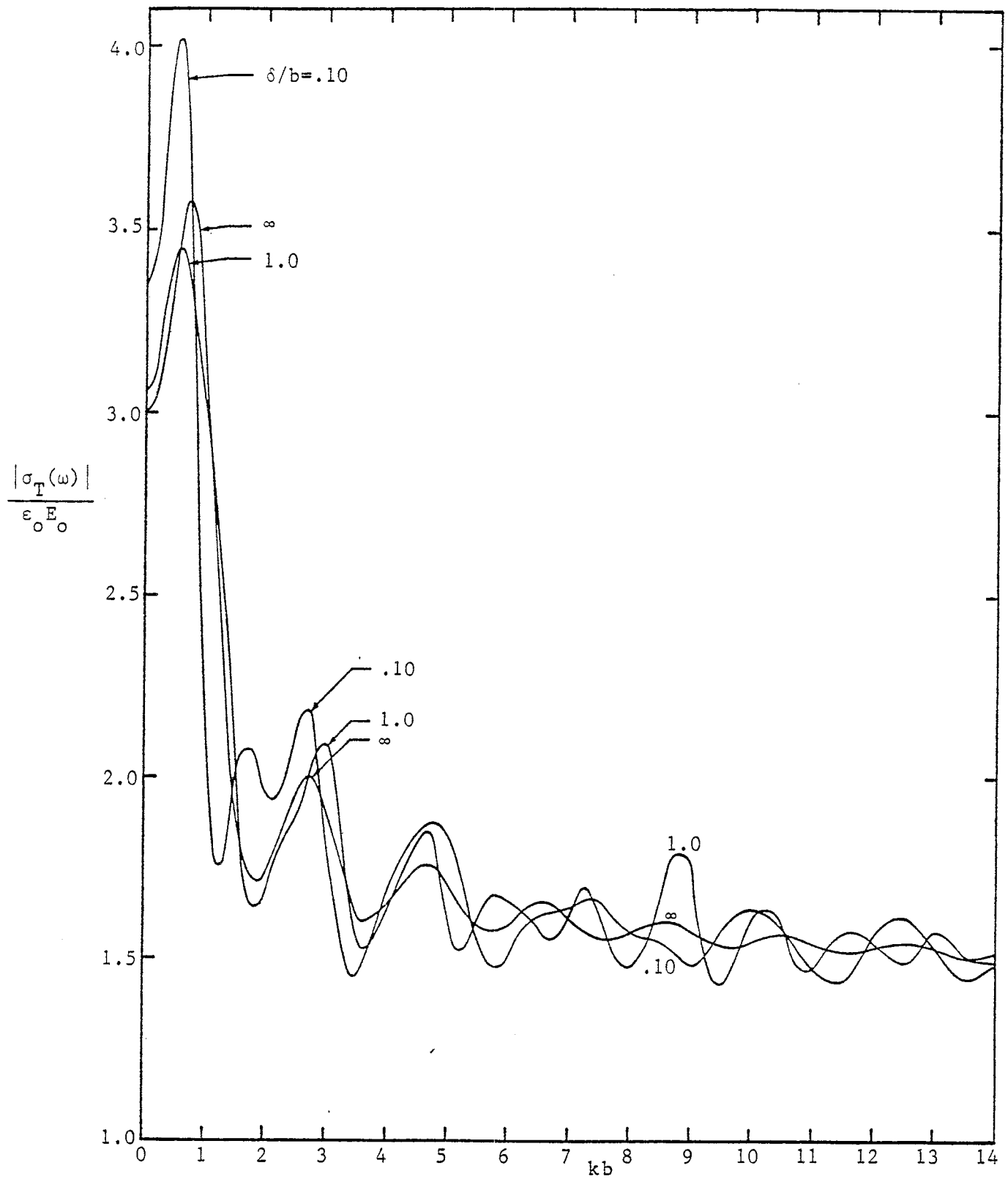


FIGURE 12

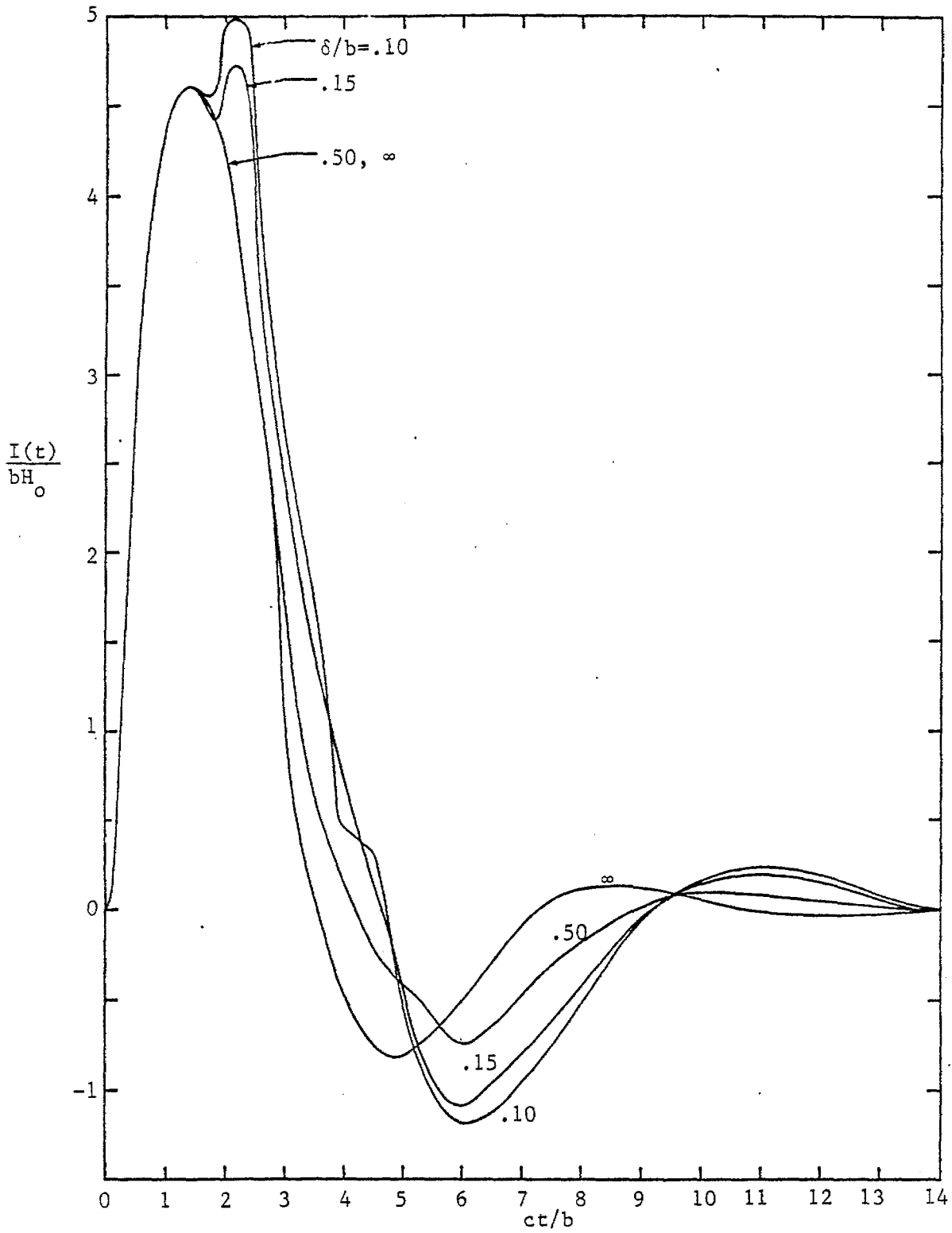


FIGURE 13

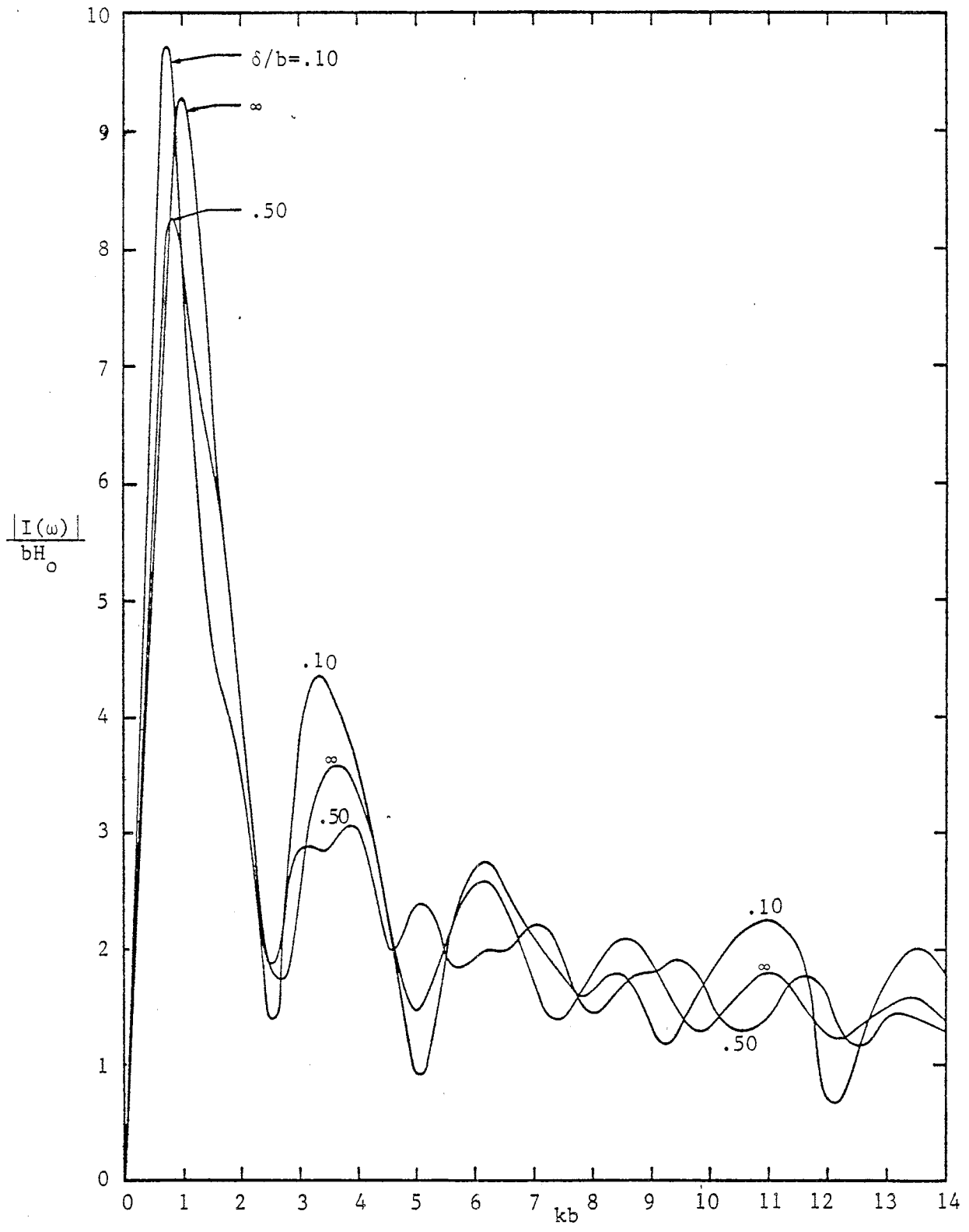


FIGURE 14

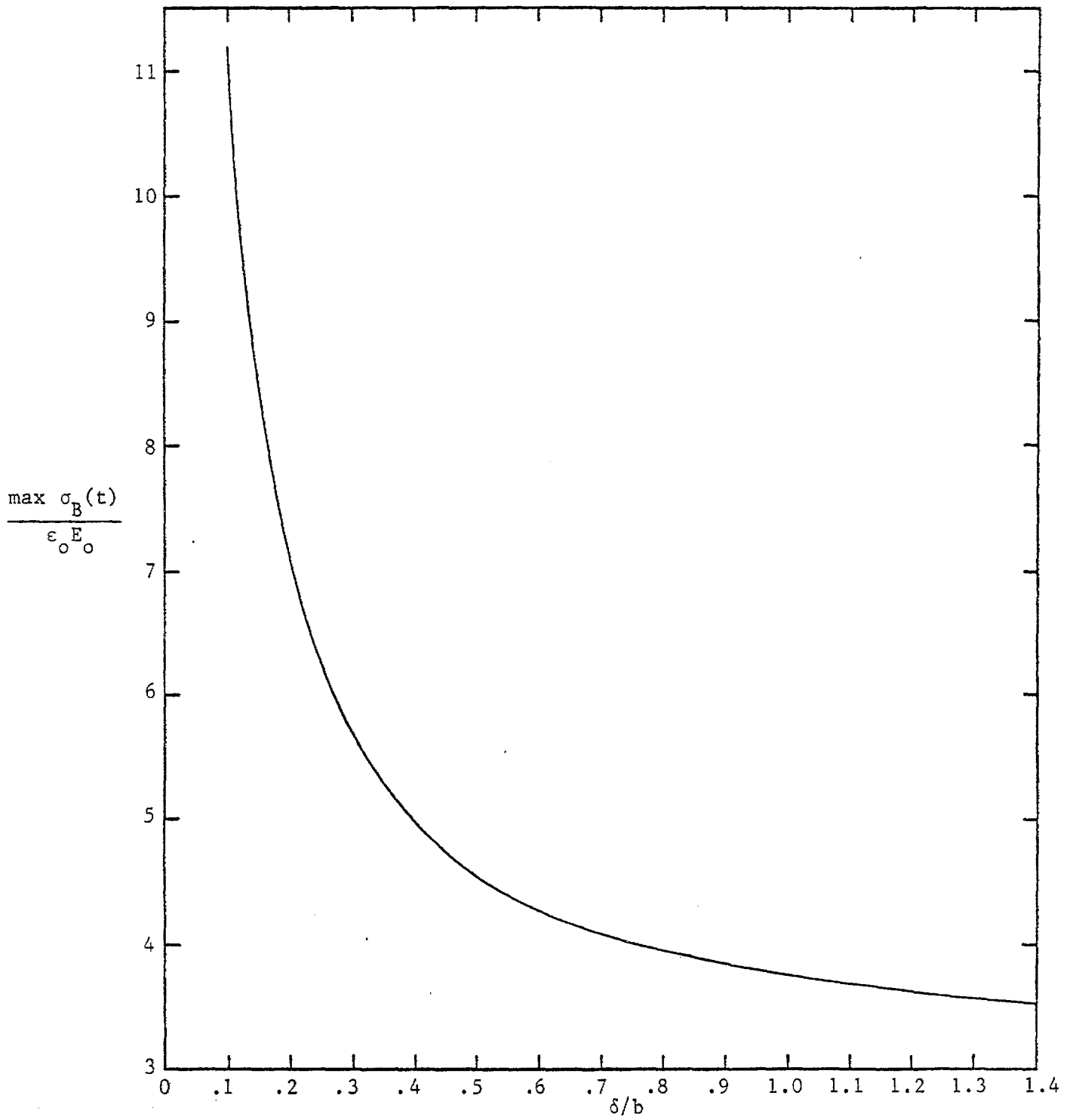


FIGURE 15

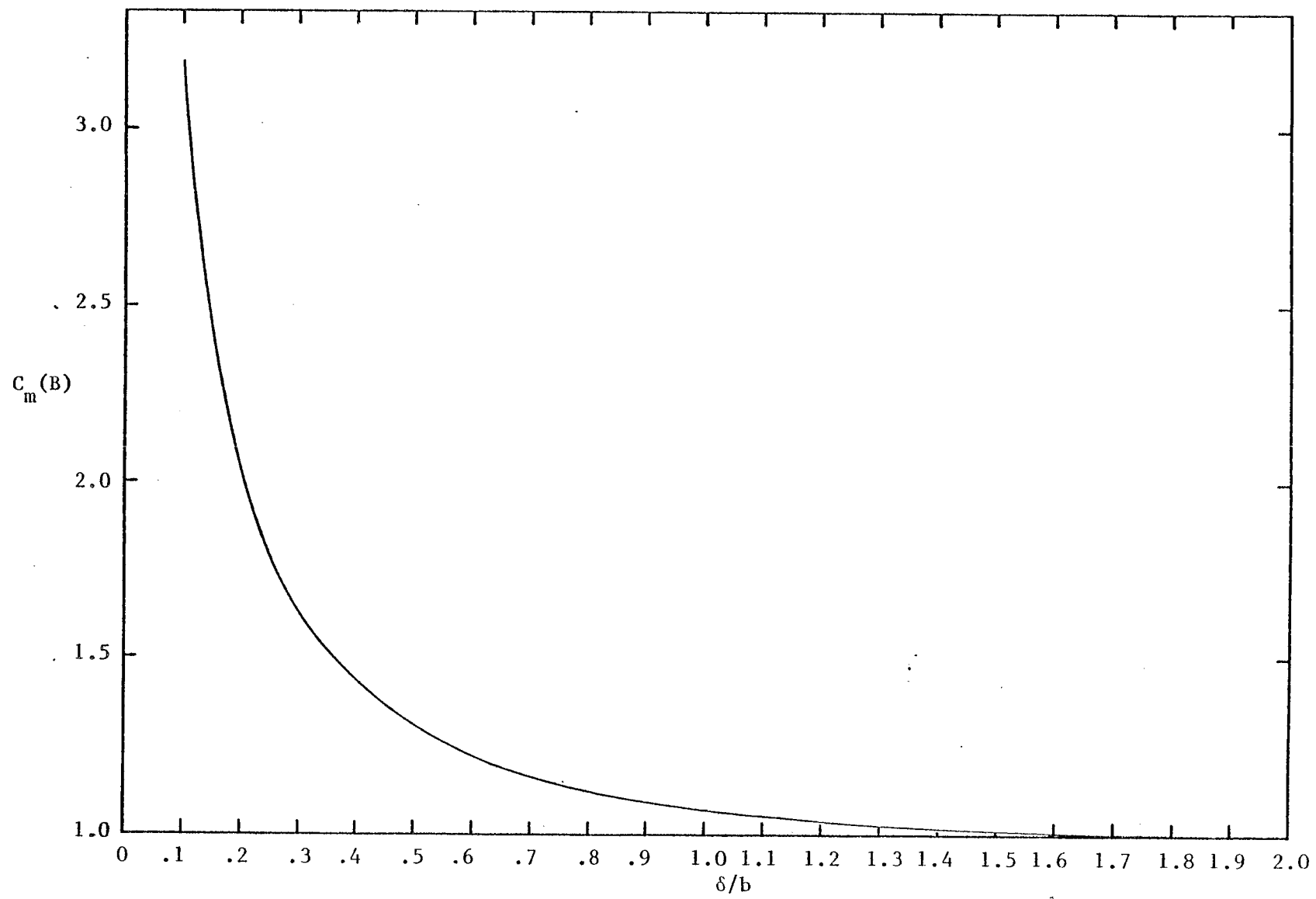


FIGURE 16

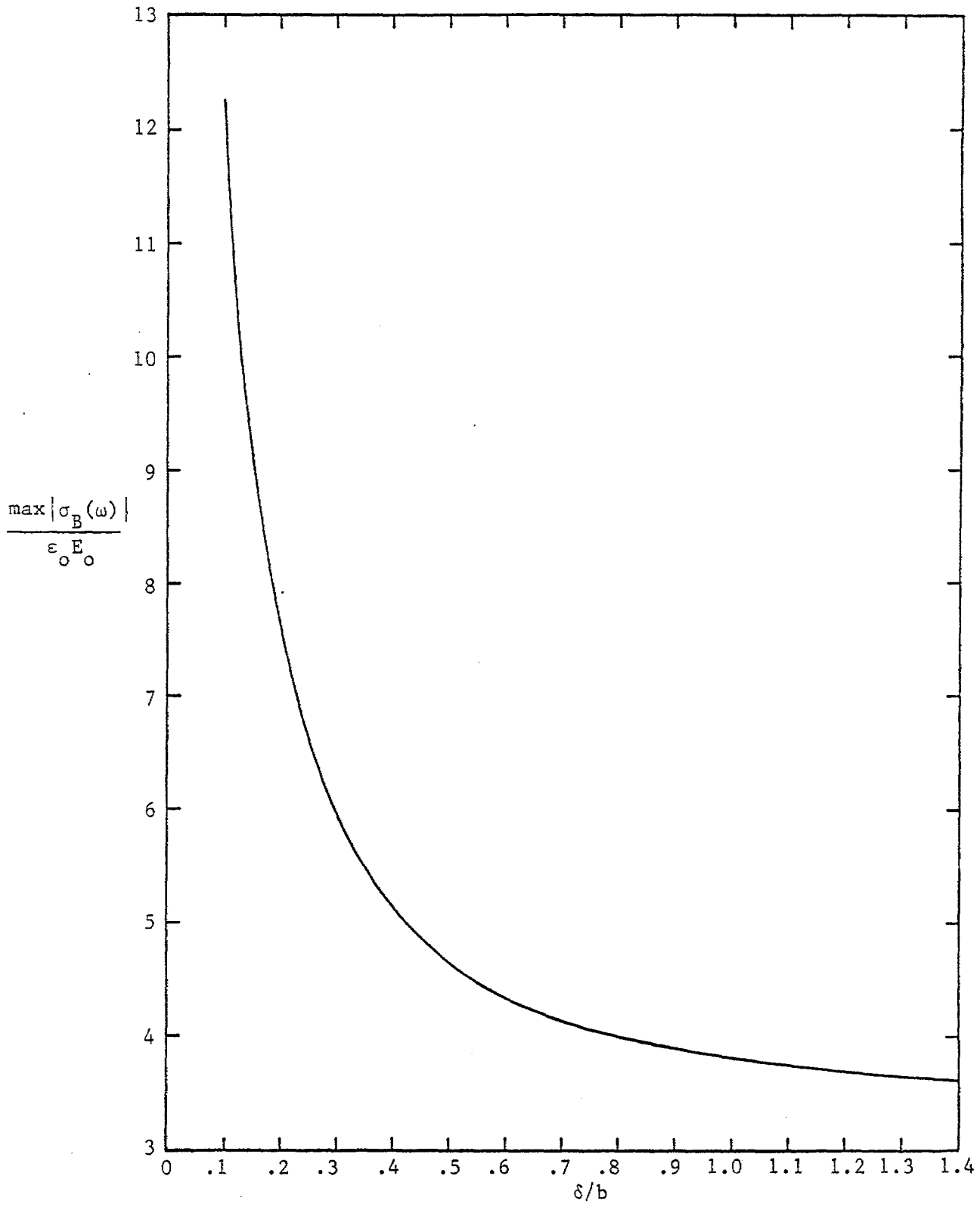


FIGURE 17

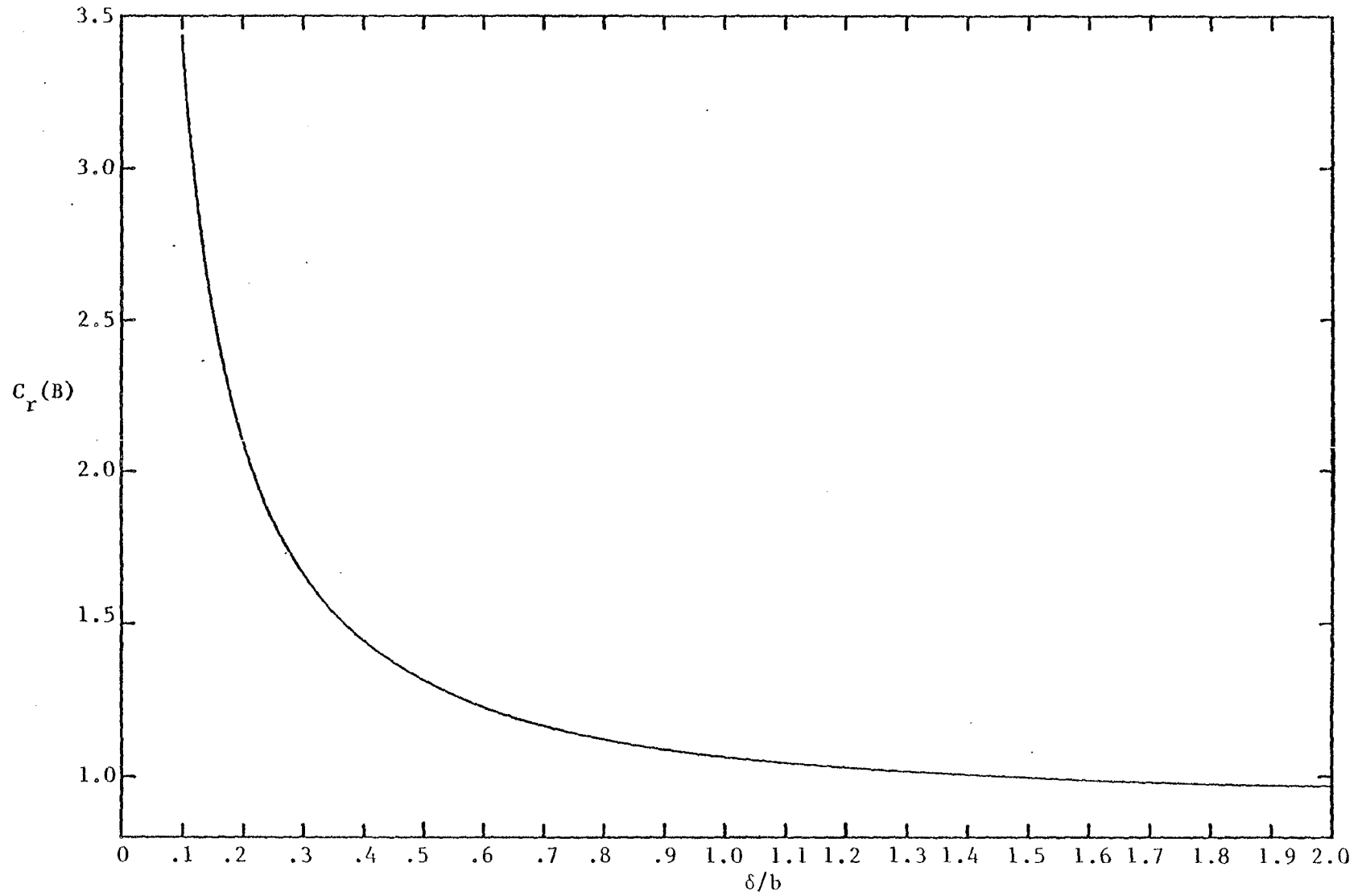


FIGURE 18

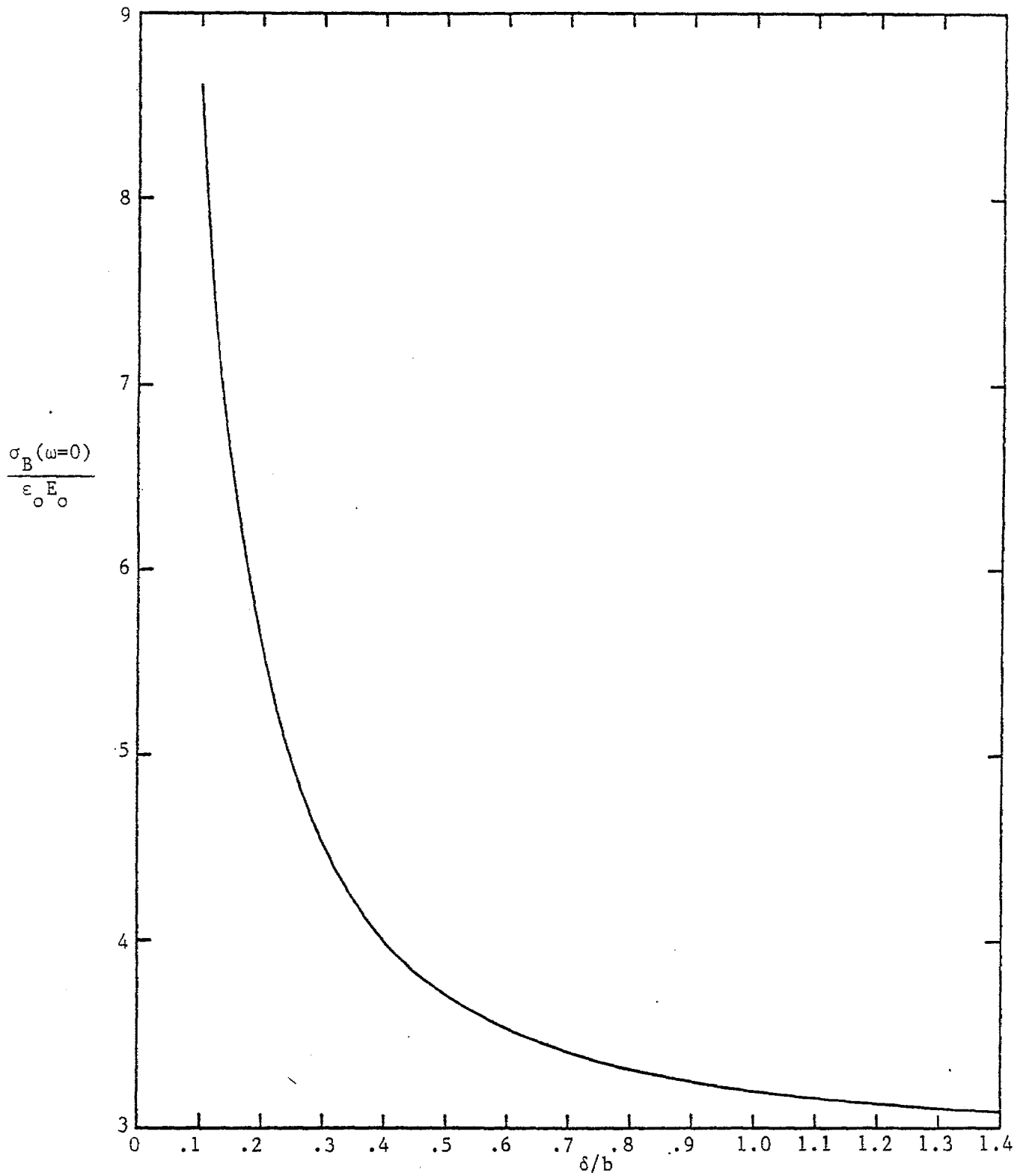


FIGURE 19

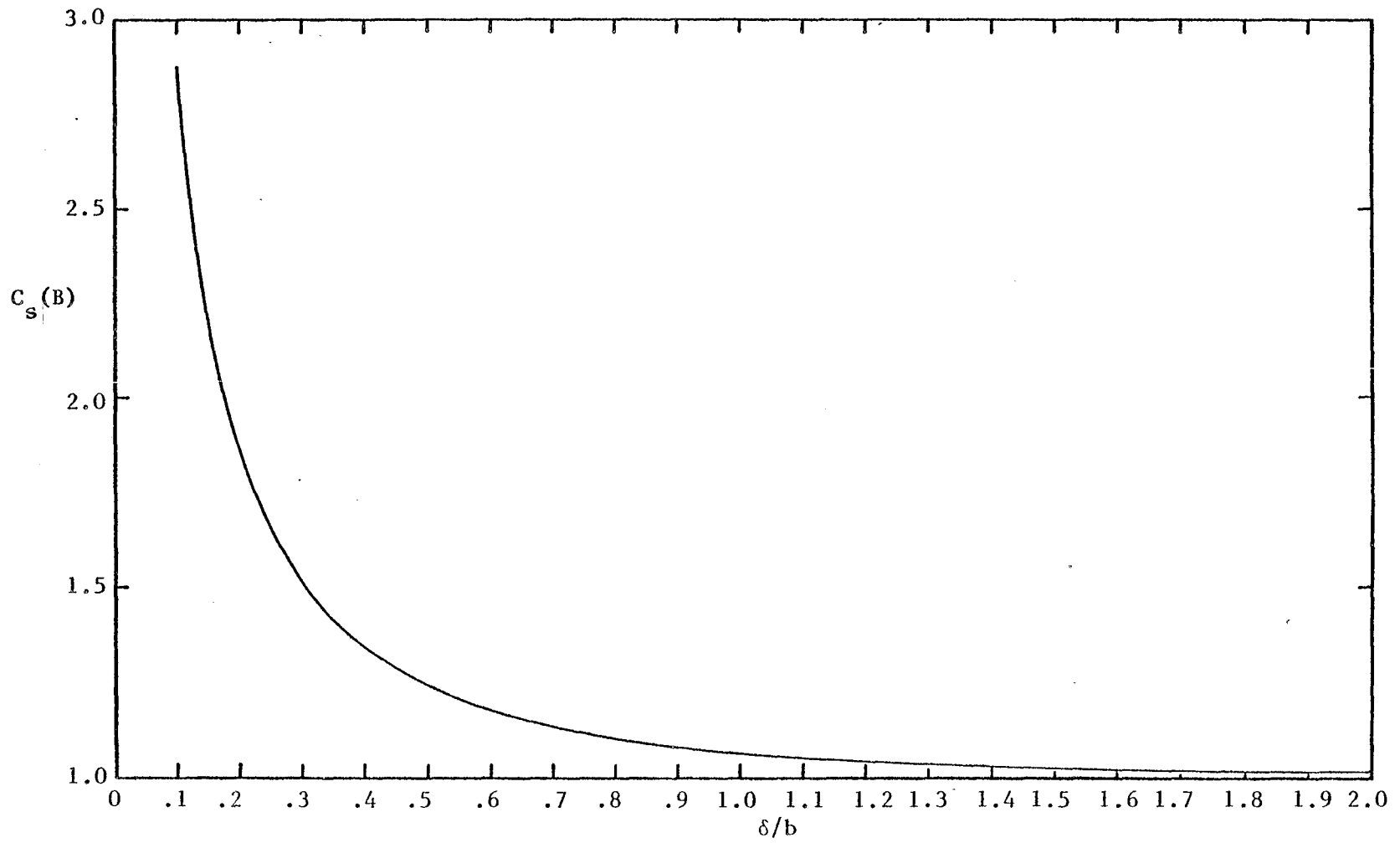


FIGURE 20

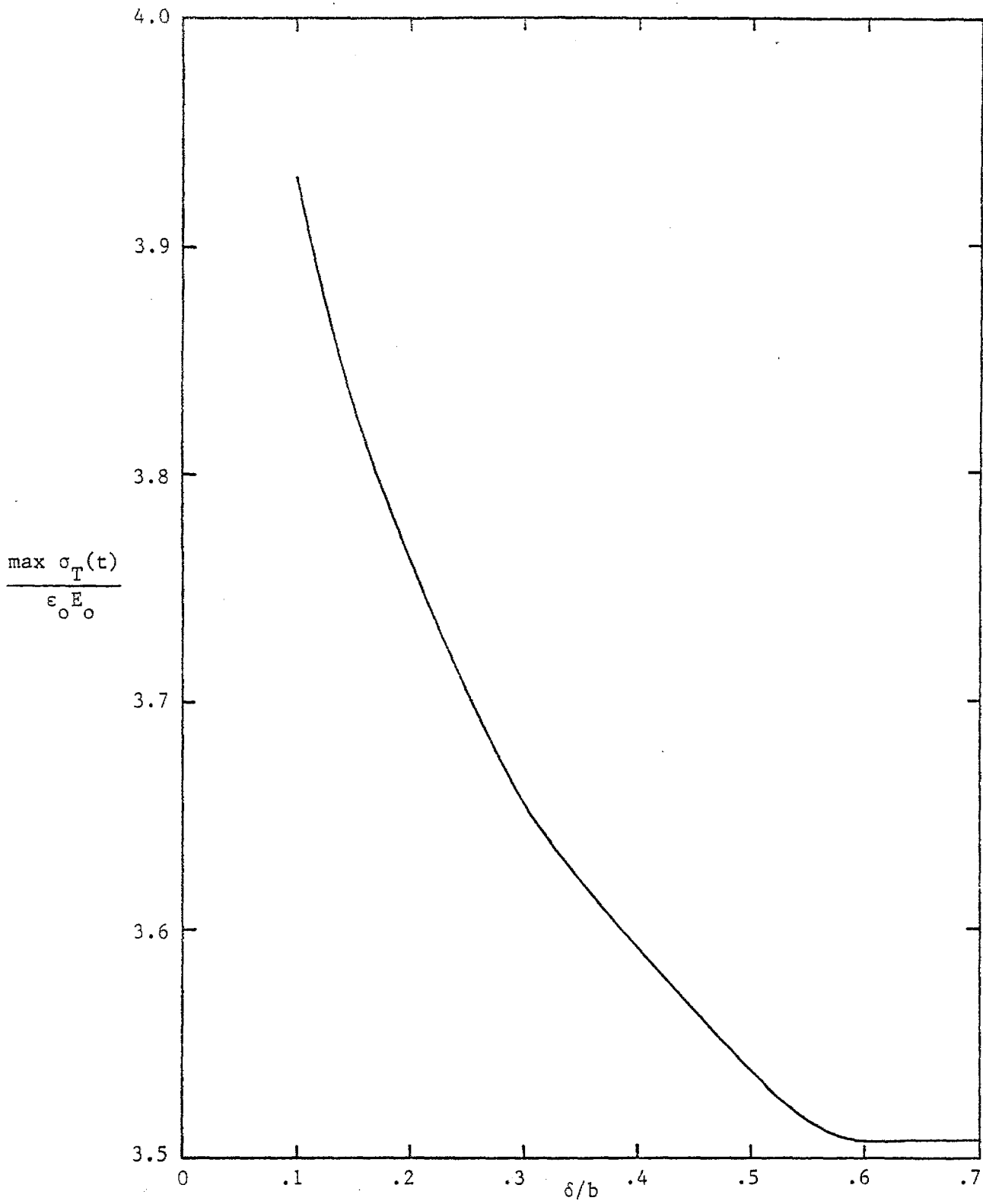


FIGURE 21

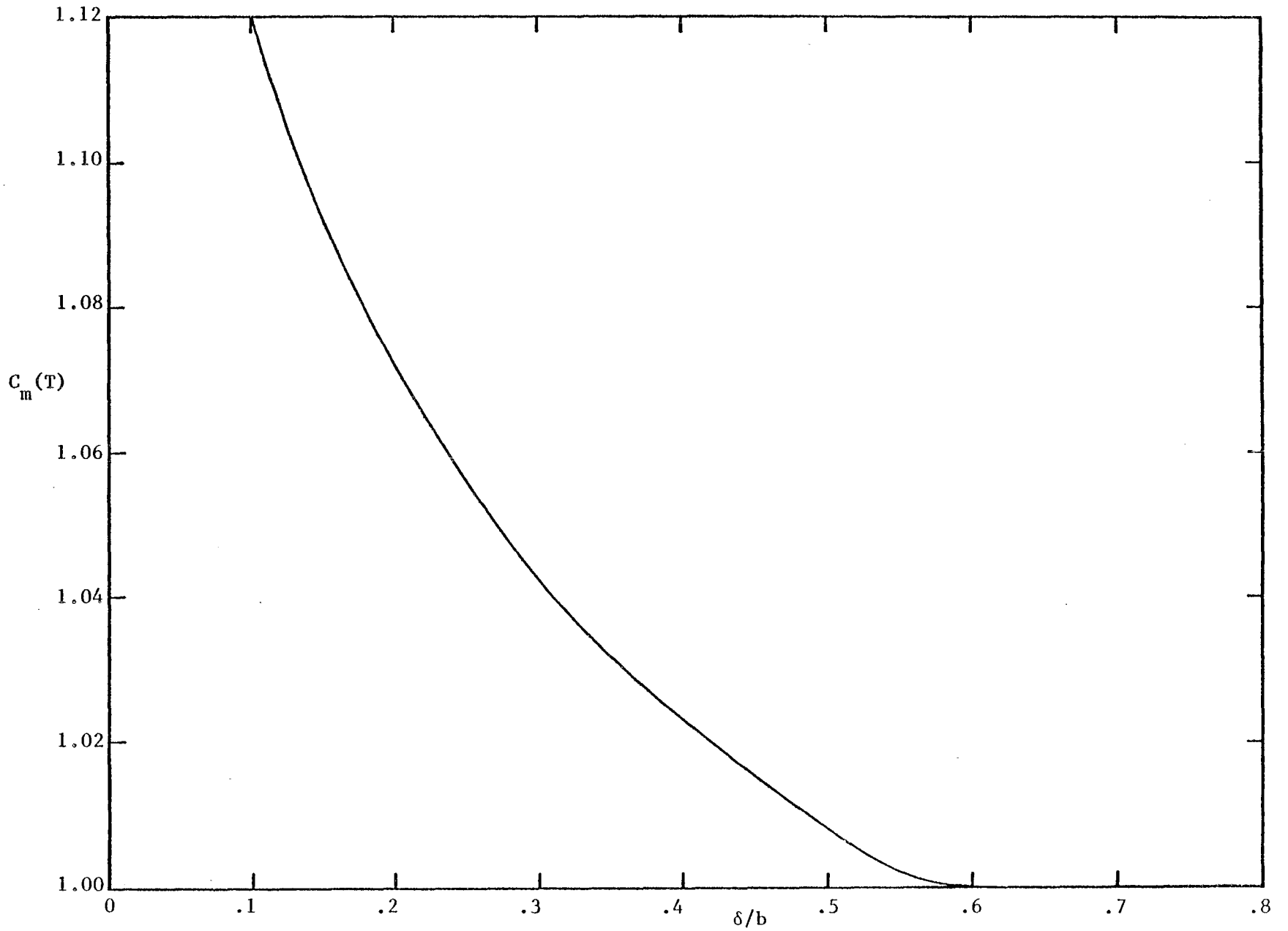


FIGURE 22

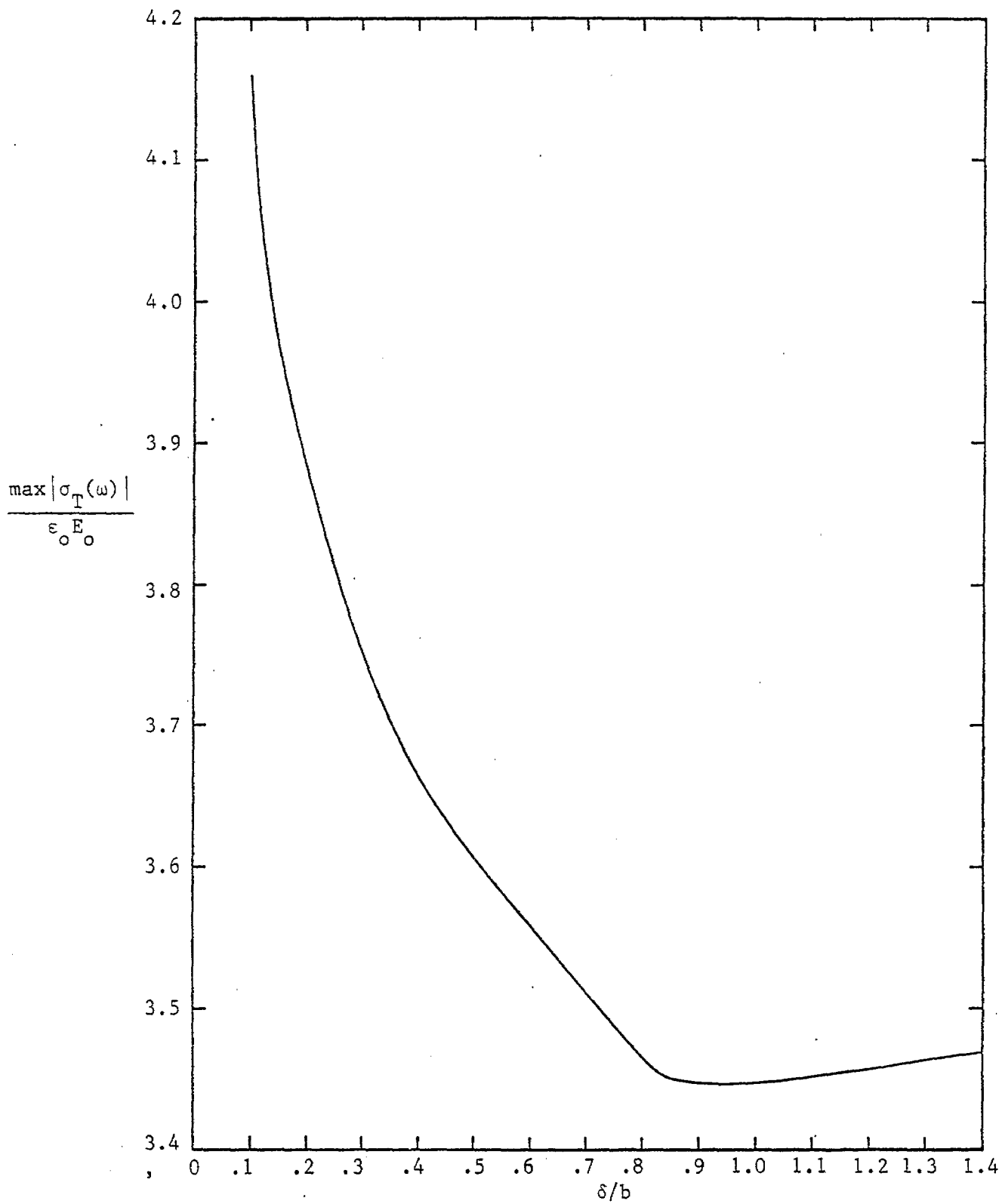


FIGURE 23

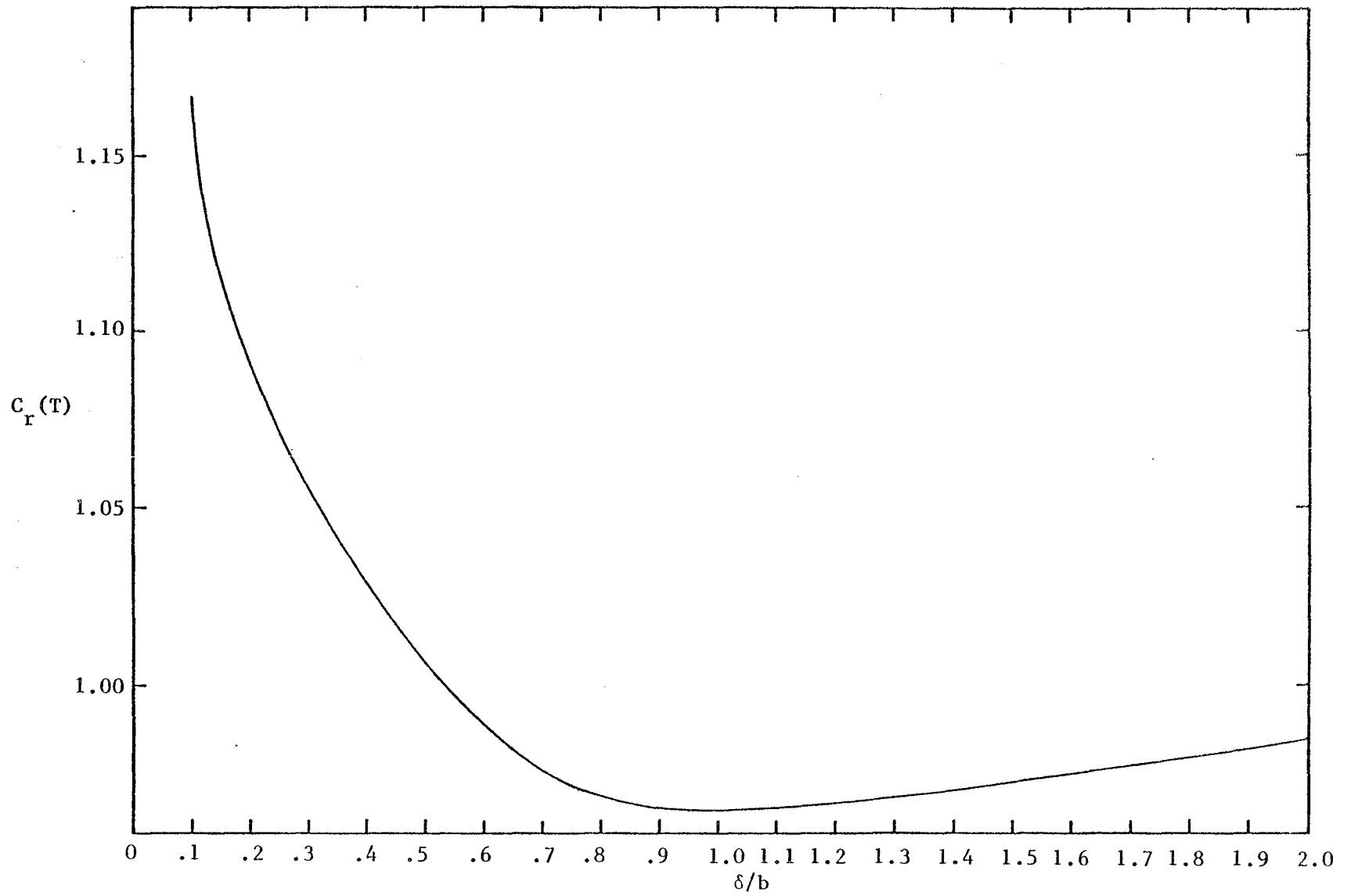


FIGURE 24

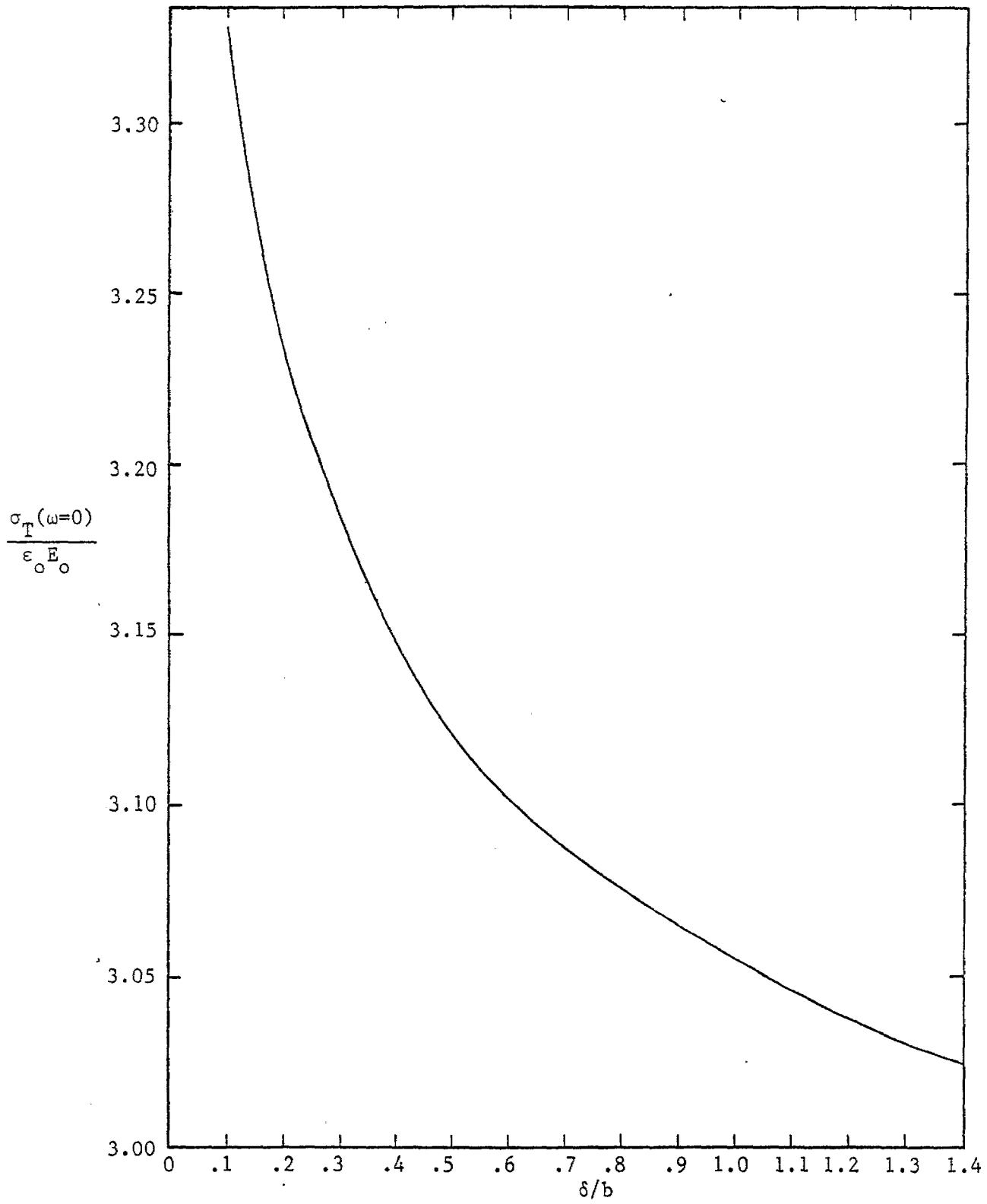


FIGURE 25

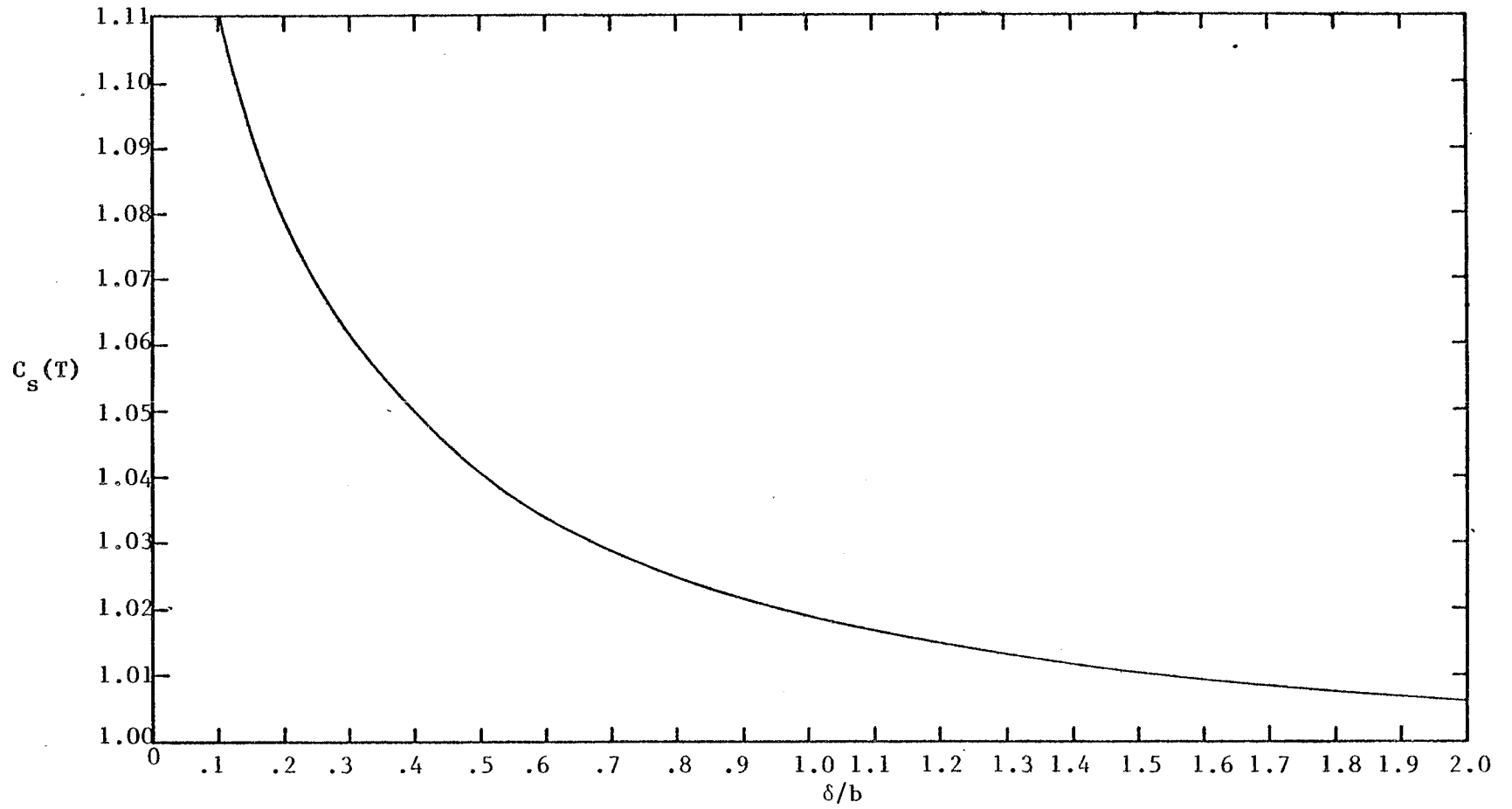


FIGURE 26

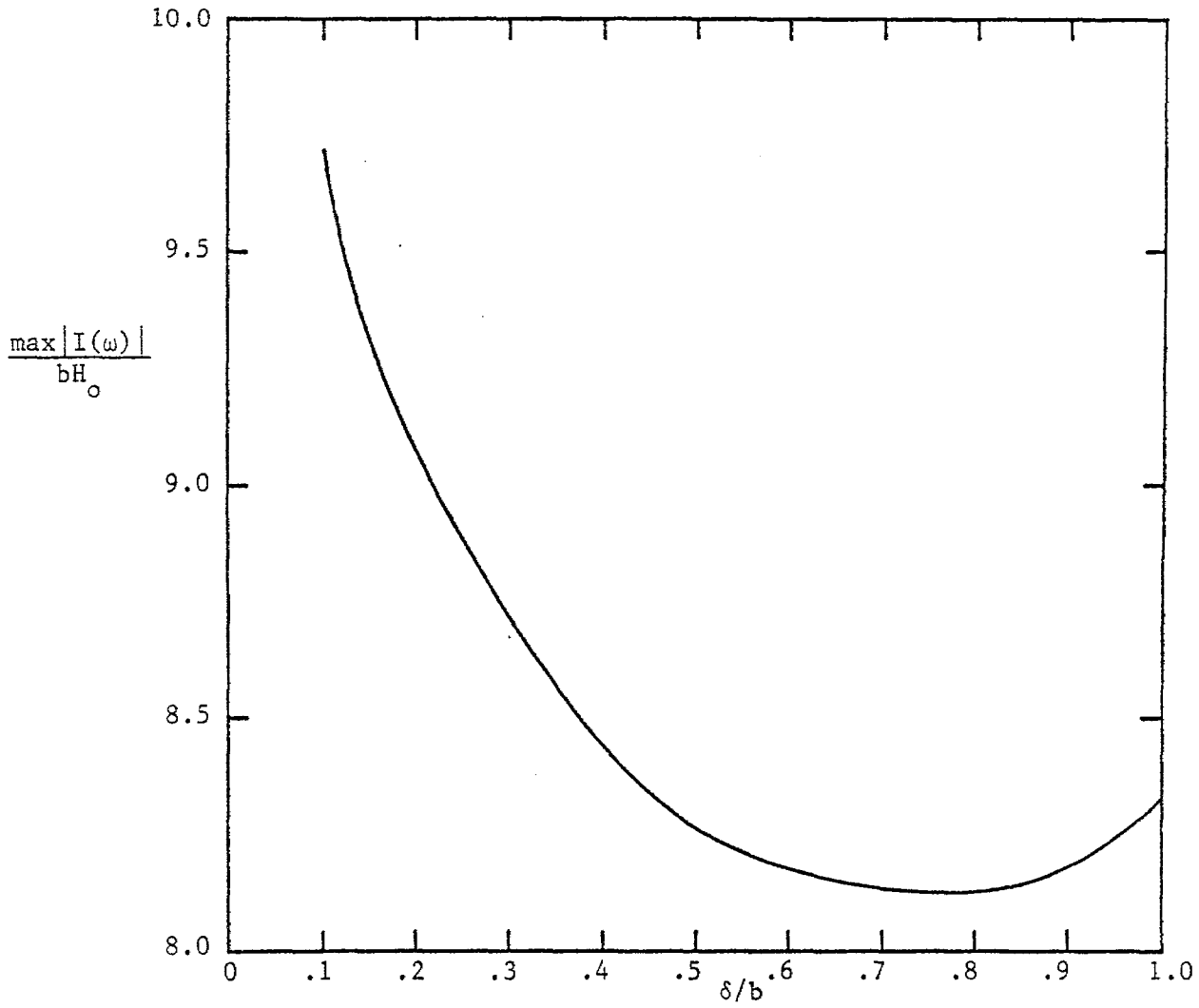


FIGURE 27

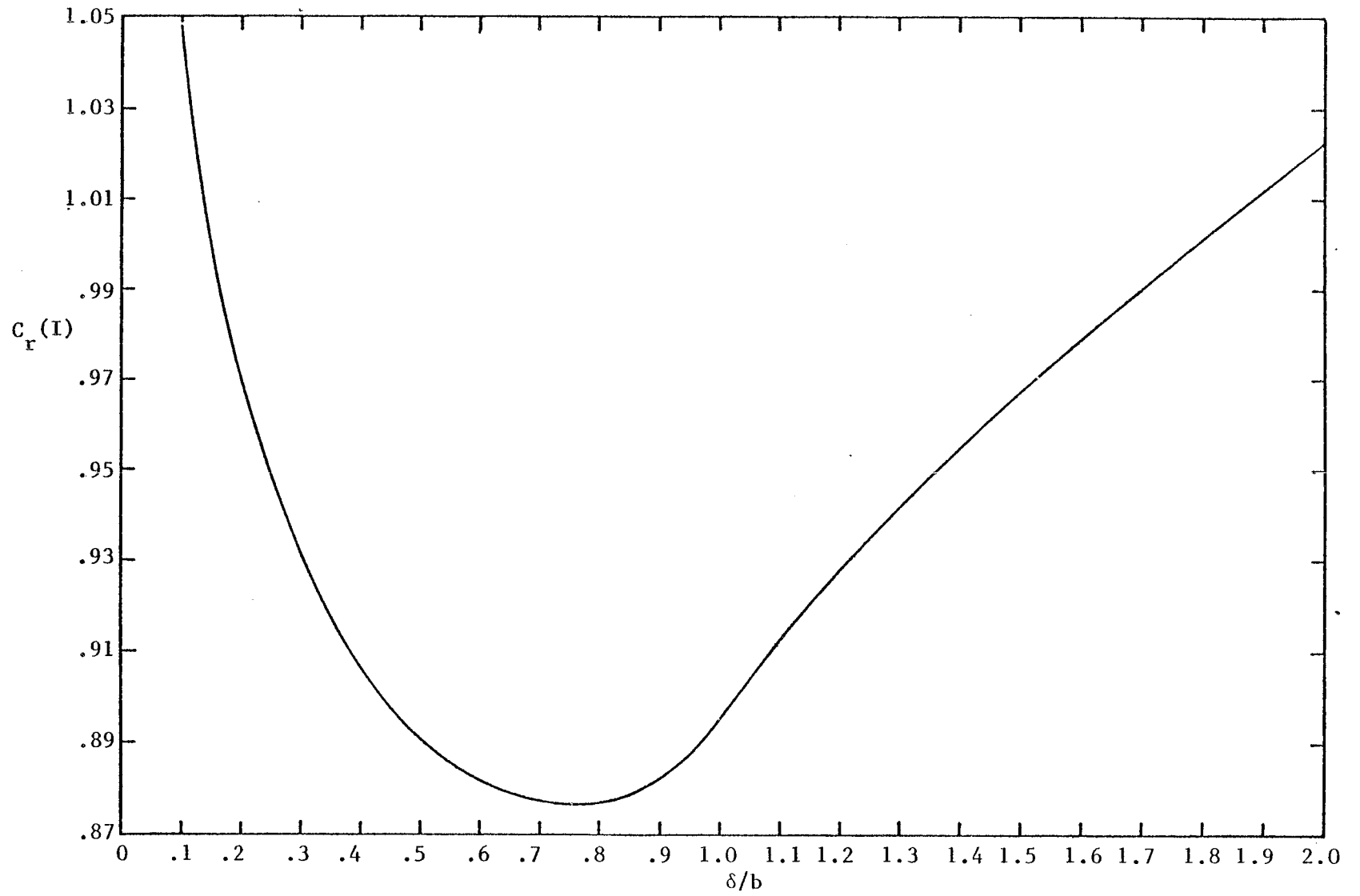


FIGURE 28

## References

1. R. W. Latham, K. S. H. Lee, and R. W. Sassman, "Minimization of Current Distortions on a Cylindrical Post Piercing a Parallel-Plate Waveguide," Sensor and Simulation Note 93, September 1969.
2. R. W. Latham and K. S. H. Lee, "Electromagnetic Interaction Between a Cylindrical Post and a Two-Parallel-Plate Simulator, I," Sensor and Simulation Note 111, July 1970.
3. K. S. H. Lee, "Electromagnetic Interaction Between a Cylindrical Post and a Two-Parallel-Plate Simulator, II (a Circular Hole in the Top Plate)," Sensor and Simulation Note 121, November 1970.
4. Lennart Marin, "A Cylindrical Post Above a Perfectly Conducting Plate, I (Static Case)," Sensor and Simulation Note 134, July 1971.
5. Lennart Marin, "A Cylindrical Post Above a Perfectly Conducting Plate, II (Dynamic Case)," Sensor and Simulation Note 136, August 1971.
6. C. D. Taylor and G. A. Steigerwald, "On the Pulse Excitation of a Cylinder in a Parallel Plate Waveguide," Sensor and Simulation Note 99, March 1970.
7. R. W. Latham, "Interaction Between a Cylindrical Test Body and a Parallel Plate Simulator," Sensor and Simulation Note 55, May 1968.
8. O. A. Germogenova, "The Scattering of a Plane Electromagnetic Wave by Two Spheres," Bull. Acad. Sci., USSR, Geophysical Series 4, 1963.
9. C. Liang and Y. T. Lo, "Scattering by Two spheres," Radio Sci., 2 (12), 1967.
10. S. Levine and G. O. Olaofe, "Scattering by Two Equal Spherical Particles," J. Colloid Institute Sci., 27 (3), 1968.
11. Ye. A. Ivanov, "Diffraction of Electromagnetic Waves on Two Bodies," Nasa Technical Translation, Nasa TT F-597, April 1970.
12. V. A. Fock, Electromagnetic Diffraction and Propagation Problems, Pergamon Press, Ltd., 1965, p. 20.
13. J. A. Cullen, "Surface Currents Induced by Short-Wavelength Radiation," Physical Review, Second Series, 109, 1958.